

2005

Growth and characterization of diamond and diamond like carbon films with interlayer

Roja Gottimukkala
University of South Florida

Follow this and additional works at: <http://scholarcommons.usf.edu/etd>

 Part of the [American Studies Commons](#)

Scholar Commons Citation

Gottimukkala, Roja, "Growth and characterization of diamond and diamond like carbon films with interlayer" (2005). *Graduate Theses and Dissertations*.

<http://scholarcommons.usf.edu/etd/2904>

This Thesis is brought to you for free and open access by the Graduate School at Scholar Commons. It has been accepted for inclusion in Graduate Theses and Dissertations by an authorized administrator of Scholar Commons. For more information, please contact scholarcommons@usf.edu.

Growth and Characterization of Diamond and Diamond like Carbon Films with Interlayer

by

Roja Gottimukkala

A thesis submitted in partial fulfillment
of the requirements for the degree of
Master of Science in Mechanical Engineering
Department of Mechanical Engineering
College of Engineering
University of South Florida

Major Professor: Ashok Kumar, Ph.D.
Frank Pyrtle, III, Ph.D.
Muhammad Rahman, Ph.D.

Date of Approval:
November 4, 2005

Keywords: Pulsed Laser Deposition, Chemical Vapor Deposition, Stress, Friction
Coefficient, Nanoindentation

© Copyright 2005, Roja Gottimukkala

DEDICATION

To God and My Family

ACKNOWLEDGEMENTS

I am indebted to everyone who helped me throughout my research work to make this work successful. I thank God and my family for their love and support, for encouraging me to seek for myself a meaningful education. Deepest thanks to my advisor, Dr. Ashok Kumar for his consistent trust and support. I would also like to express my sincere gratitude to thesis committee members, Dr. Frank Pyrtle, III and Dr. Muhammad Rahman for being on the committee. Just a word 'thanks' is not adequate to acknowledge the help and encouragement given by my friend Harish during the research work. Thanks are due to Raghu, for his encouragement and valuable suggestions. Thanks are in order for all my colleagues and my friends (especially Sriram and Swetha) for their encouragement and moral support during the research period.

TABLE OF CONTENTS

LIST OF TABLES	iii
LIST OF FIGURES	iv
ABSTRACT	vi
CHAPTER 1 INTRODUCTION TO DIAMOND AND DIAMOND RELATED MATERIALS	1
1.1 Different Forms of Carbon	1
1.2 Diamond	2
1.2.1 History of Diamond	4
1.2.2 Structure of Diamond	5
1.2.3 Properties of Diamond	6
1.2.4 Growth of Diamond	8
1.2.5 Deposition Techniques	8
1.2.5.1 Hot Filament Assisted CVD	8
1.2.5.2 DC Plasma Assisted CVD	9
1.2.5.3 RF Plasma Assisted CVD	9
1.2.5.4 Microwave Plasma Assisted CVD	10
1.2.5.5 Electron Cyclotron Resonance –MPACVD	10
1.2.6 Applications of Diamond Films and Coatings	10
1.3 Diamond-like Carbon (DLC) Films	11
1.3.1 History of Diamond-like Carbon Films	12
1.3.2 Structure of Diamond-like Carbon Films	13
1.3.3 Mechanical Properties	14
1.3.4 Deposition Techniques	15
1.3.4.1 Filtered Cathodic Arc Deposition	15
1.3.4.2 Pulsed Laser Deposition	16
1.3.4.3 Magnetron Sputtering	16
1.3.5 Applications	17
1.4 Literature Review	17
1.5 Overview of the Thesis	19
CHAPTER 2 EXPERIMENTAL TECHNIQUES	21
2.1 Diamond-like Carbon Films	22
2.1.1 Pulsed Laser Ablation	22

2.1.2	Experimental Procedure	26
2.2	Diamond Films	27
2.2.1	CVD Deposition Technique	27
2.2.1.1	Microwave Plasma Assisted CVD	30
2.2.2	Experimental Procedure	31
CHAPTER 3	STRUCTURAL AND MECHANICAL CHARACTERIZATION	32
3.1	Raman Spectroscopy	32
3.2	Nanoindentation	34
3.3	Nanoindentation Data Analysis	36
3.3.1	Doerner and Nix Method	36
3.3.2	Oliver and Pharr Method	36
3.3.3	Basic Equations Involved	36
3.4	X-Ray Diffraction	39
3.5	Friction Test	41
3.5.1	Description of UMT	42
CHAPTER 4	RESULTS AND DISCUSSION	44
4.1	Amorphous Carbon Films without Interlayer	44
4.1.1	Raman Spectroscopy	45
4.1.2	Nanoindentation	48
4.2	Tetrahedral Amorphous Carbon Films with Interlayer	50
4.2.1	Raman Spectroscopy	51
4.2.2	Nanoindentation	56
4.2.3	Friction Test	61
4.3	Diamond	62
4.3.1	Raman Spectroscopy	63
4.3.2	X-ray Diffraction	64
CHAPTER 5	CONCLUSIONS AND RECOMMENDATIONS	66
REFERENCES		68

LIST OF TABLES

Table 1.1	Properties of Various Forms of Carbon	2
Table 1.2	Properties of Diamond	3
Table 1.3	Properties of Diamond Compared to Other Semiconductors	7
Table 2.1	Properties of Diamond and DLC Materials	21
Table 2.2	History of CVD Diamond	30
Table 4.1	Residual Stress in the Tetrahedral Amorphous Carbon Films Obtained from Raman Spectra	47
Table 4.2	Hardness and Young's Modulus for Tetrahedral Amorphous Carbon Films Deposited at Various Temperatures	49
Table 4.3	Reduction in Stress (GPa) Obtained from Raman Analysis	55
Table 4.4	Summarized Results Obtained from Nanoindentation for Layered Tetrahedral Amorphous Carbon Films	57
Table 4.5	Friction Coefficient of Layered ta-C Films	61
Table 4.6	Increase in Stress (GPa) Obtained from Raman Analysis	64

LIST OF FIGURES

Figure 1.1	Structure of Diamond	6
Figure 1.2	Ternary Phase Diagram of DLC Films Showing sp^3 , sp^2 , and H Contents	14
Figure 2.1	Schematic Representation of Laser-Target Interactions	23
Figure 2.2	PLD System at USF	25
Figure 3.1	Renishaw Raman Spectrometer at USF	34
Figure 3.2	Plot of Load vs Displacement Data	35
Figure 3.3	a) Schematic of Indenter and Specimen Geometry b) Load Displacement Curve	38
Figure 3.4	Schematic of Nanoindenter XP	39
Figure 3.5	X-Ray Diffraction	41
Figure 3.6	Universal Micro Tribometer with PC Based Feed Back Control	42
Figure 4.1	Raman Spectra of the Tetrahedral Amorphous Carbon Films Deposited at Different Temperatures	45
Figure 4.2	Modulus vs Displacement Plot of Tetrahedral Amorphous Carbon Films Deposited at Different Temperatures	49
Figure 4.3	Hardness vs Displacement Plot of Tetrahedral Amorphous Carbon Films Deposited at Different Temperatures	50
Figure 4.4	Raman Spectra of ta-C Film with Ta as Interfacial Layer	52
Figure 4.5	Raman Spectra of ta-C Film with Different Interlayers Deposited at 100°C	53
Figure 4.6	Raman Spectra of ta-C Film with Different Interlayers Deposited at 300°C	53
Figure 4.7	Raman Spectra of ta-C Film with Different Interlayers Deposited at 600°C	54

Figure 4.8	Reduction in Stress vs Interlayer Material at Different Temperatures	56
Figure 4.9	Modulus vs Displacement Plot of ta-C Film with the Interlayers Deposited at 100°C	58
Figure 4.10	Hardness vs Displacement Plot of ta-C Film with the Interlayers Deposited at 100°C	58
Figure 4.11	Modulus vs Displacement Plot of ta-C Film with the Interlayers Deposited at 300°C	59
Figure 4.12	Hardness vs Displacement Plot of ta-C Film with the Interlayers Deposited at 300°C	59
Figure 4.13	Modulus vs Displacement Plot of ta-C Film with the Interlayers Deposited at 600°C	60
Figure 4.14	Hardness vs Displacement Plot of ta-C Film with the Interlayers Deposited at 600°C	60
Figure 4.15	Raman Spectra of Diamond Films with Different Interfaces	64
Figure 4.16	XRD of original substrate and TiC- diamond film	65

GROWTH AND CHARACTERIZATION OF DIAMOND AND DIAMOND LIKE CARBON FILMS WITH INTERLAYER

Roja Gottimukkala

ABSTRACT

Diamond and diamond-like carbon films, with their exceptionally good mechanical, chemical, and optical properties, are the best materials as protective hard coatings for electronic devices and cutting tools. The biocompatibility of these materials makes it suitable for bone implants. The wide range applications of these films are hindered because of the high compressive stresses developed during the deposition. Use of carbide and nitride interfacial layers has emerged as one of the methods to reduce the compressive stresses.

The present research focuses on the study of different materials as the interfacial layers for diamond and tetrahedral amorphous carbon films. For tetrahedral amorphous carbon AlN, Ta, TiN, TiC, TaN and W were investigated as the interlayer materials. The interlayer was deposited at different substrate temperatures to study the temperature induced changes in the residual stress. The tetrahedral amorphous carbon with TiN interlayer deposited at 300°C and 600°C exhibited a maximum reduction in the stress.

TiN and TiC were deposited as interlayer for the diamond films on Ti-6Al-4V alloy. TiC has improved the adhesion of diamond with the substrate and exhibited less compressive stresses compared to TiN.

CHAPTER 1

INTRODUCTION TO DIAMOND AND DIAMOND RELATED MATERIALS

1.1 Different Forms of Carbon

Carbon is the sixth most abundant material that exists in about million different compounds in different forms. Diamond, graphite, fullerene, and amorphous carbon are the four known allotropes of carbon. The atomic arrangement makes the carbon to exist in different forms. Graphite is soft and slippery in contrast to diamond which is the hardest material known to man. Diamond is an abrasive whereas graphite is a good lubricant because the graphite layers stick to each other. These extremely diverse properties can be attributed to the type of bonding between carbon atoms. Diamond has sp^3 hybridized orbital in which four carbon atoms form covalent bonding with the adjacent atoms resulting in a tetrahedral structure. Graphite has sp^2 bonding where three carbon atoms form a trigonal structure in a plane and π bonding exists between the layers. Graphite has low coefficient of friction because of this π bonding between the layers. The other type of bonding is sp^1 where in the two valence electrons of carbon atom form bonds in a plane and the other two electrons form the π bond. Diamond-like carbon has a mixture of sp^3 and sp^2 bonding. It is hard to make diamond because carbon tends to be in graphite form under normal conditions as it is more stable. Even though graphite is the stable form, diamond once formed would never

alter to graphite. Amorphous carbon films exhibit mechanical, electrical and optical properties similar to that of diamond but they lack the crystalline structure.

Table 1.1 Properties of Various Forms of Carbon[7]

	Density (g/cm ³)	Hardness(GPa)	% sp ³	at% H	Band Gap(eV)
Diamond	3.515	100	100		5.5
Graphite	2.267		0		~0.04
Glassy C	1.3-1.55	2-3	~0		0.01
a-C,evap.	1.9-2.0	2-5	1		0.4-0.7
a-C,sputt	1.9-2.4	11-15	2-5		0.4-0.7
a-C:H, hard	1.6-2.2	10-25	30-60	10-40	0.8-1.7
a-C:H,soft	0.9-1.6	<5	50-80	40-65	1.6-4
Polyethylene	0.92	0.01	100	67	6
ta-C	3.0	55-65	mainly	<1	

1.2 Diamond

Diamond, the marvel material, represents the extreme value for any material property. The word "diamond" derives from the Greek word *adamas*, which means "impossible to tame". Diamond is rare in nature because carbon reacts with many elements forming different compounds and graphite formation is faster than diamond under ordinary conditions. Owing to its high hardness, diamond is used in grinding, polishing and making weapons. Diamond studded rotary drill bits and saws were used to dig oil wells

and bore holes through hard rocks. These are only a few applications of diamond. Naturally available diamond is difficult to be engineered into different physical configurations. Hence, the synthesis of diamond as a thin film or a coating has gained interest in both research and industry. Though diamond can be found from different sources, about 90 tons of single crystal diamond are synthetically made from graphite at high temperatures and pressures every year, and are cheaper compared to natural diamond. Polycrystalline diamond can be sintered and the diamond thin films are grown using the most promising chemical vapor deposition technique. Though the cost of these films is more than naturally occurring diamond, their application can be justified economically.

Basic properties of diamond are given in Table 1.2

Table 1.2 Properties of Diamond

Property	Value
Crystal structure	FCC (sp^3 bonded, tetrahedral)
Atomic density	$1.76 \times 10^{23} \text{ cm}^{-3}$
Lattice constant	3.567 \AA
Hardness	$1.0 \times 10^4 \text{ kg/mm}^2$
Tensile strength	$>1.2 \text{ GPa}$
Compressive strength	$>110 \text{ GPa}$
Coefficient of friction	0.03
Sound velocity	$1.8 \times 10^4 \text{ ms}^{-1}$
Density	3.52 gcm^{-3}
Young's Modulus	1.22 GPa
Poisson's Ratio	0.2
Thermal expansion coefficient	$1.1 \times 10^{-6} \text{ k}^{-1}$
Thermal conductivity	2500 W/m-k

Table 1.2 (continued)

Thermal shock parameter	$3.0 \times 10^8 \text{ Wm}^{-1}$
Debye temperature	2200 K
Optical index of refraction(at 591 nm)	2.41
Optical transmittivity	225 nm (UV) to long IR (> 25 μm),IR absorption band from 2-7 μm
Loss tangent at 40 Hz	6.0×10^{-4}
Dielectric constant	5.7
Dielectric strength	$1.0 \times 10^{-7} \text{ Vcm}^{-1}$
Electron mobility	$2200 \text{ cm}^2(\text{Vs})^{-1}$
Hole mobility	$1600 \text{ cm}^2(\text{Vs})^{-1}$
Electron saturated velocity	$2.7 \times 10^7 \text{ cms}^{-1}$
Hole saturated velocity	$1.0 \times 10^7 \text{ cms}^{-1}$
Work function	Negative for [111] surface -1 eV
Bandgap	5.45 eV
Resistivity	$10^{13}\text{-}10^{16} \Omega\text{-cm}$

1.2.1 History of Diamond

The existence of diamond can be dated back to biblical times. It is believed that they are first found in the river basins of Godavari and Krishna in India. Though it is a widely known fact that diamond is famous as a precious stone in jewelry, it was shown that the diamond had many other applications. It was first used in grinding and polishing. But unfortunately, the naturally available diamond cannot be engineered into different physical configurations. The saga of the efforts to produce synthetic diamond started in early 1950's. The first fruitful effort to grow diamond at low pressures was by William Eversole of Union Carbide Corporation in 1952. He produced diamond on a diamond

seed crystal using carbon monoxide as source gas. No later, General Electric came up with the idea of growing diamond at high temperature and high pressure in 1955. In 1960's Angus proposed the Chemical Vapor Deposition (CVD) technique as the most feasible method for growing diamond thin films. The diamond obtained was in metastable phase. They found that the diamond could be efficiently grown in excessive hydrogen. Though the molecular hydrogen ceased the growth of the graphite to a good extent, the need for removing the deposited graphite was accomplished by atomic hydrogen. Gardener first generated the atomic hydrogen using a hot tungsten filament and this was used to etch the graphite deposits. In 1970's Deryagin reported the growth of diamond films on non diamond substrates [24]. In 1980, researchers at National Institute for Research in inorganic Materials (NIRIM) used a hot filament to activate methane and hydrogen. The success of NIRIM in growing metastable diamond at a rapid rate augmented the interest of many groups in the low pressure diamond growth.

1.2.2 Structure of Diamond

The structure of diamond, to which the various extreme properties can be attributed, is shown in Figure 1.1 All the important applications of diamond have the most common face centered cubic crystal with four atoms spaced at a quarter of a cube diagonal. Diamond also has a hexagonal structure known as lonsdaleite, mostly found in meteorites.

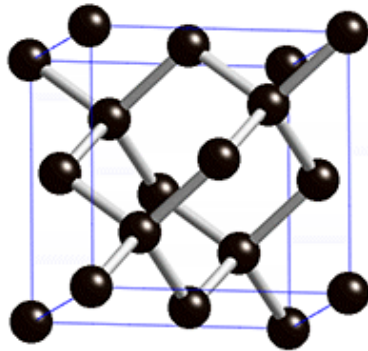


Figure 1.1 Structure of Diamond

1.2.3 Properties of Diamond

Hardness is the most important characteristic of diamond that makes it an ideal material for cutting and grinding tools. The hardness of the diamond is due to its atomic arrangement. Different tools like drill bits, wire drawing dies and extrusion dies are coated with diamond films but care should be taken regarding the adhesion of these films. Because the diamond reacts and dissolves in ferrous materials, they are not applied to ferrous materials. Its other properties include high thermal conductivity, chemical inertness, and low coefficient of thermal expansion, high yield stress, optical transparency, exhibits excellent tribological properties and electrical properties. Though natural diamond exhibits exceptional properties, it cannot be engineered to all desired combinations of these properties. Diamond as a thin film or coating has potential to exhibit more combinations for specific applications. The high hardness and optical transmissivity of diamond makes it an ideal material for radomes and windows. Diamond with large dielectric constant, low mass density and low coefficient of thermal expansion is good to use as a capacitor material. The high thermal conductivity of diamond makes it the best choice for heat spreaders and heat exchangers. Most of its applications lie in the

electronic devices. Diamond films are used to coat magnetic tapes and diamond fibers are used in composites for reinforcement. Due to high band gap of 5.5eV, dipoles are not present in the diamond and hence the spectral transmission is wide.

Few fundamental properties of other competing materials are listed in Table 1.3. Though materials like silicon, germanium and silver have the same structure, it can be observed that most of the properties of diamond are much better than its competitors.

Table 1.3 Properties of Diamond Compared to Other Semiconductors

Property	Silicon	SiC	Diamond
Lattice constant (Å)	5.43	4.358 (for β-SiC)	3.567
Thermal expansion (in 10 ⁻⁶ °C)	2.6	4.7	1.1
Density(gcm ⁻³)	2.328	3.216	3.515
Melting point(in °C)	1420	2540	4000
Max Operating Temp (C)	225		1900
Bandgap(eV)	1.1	3.0	5.45
Saturated electron velocity(X 10 ⁷ cms ⁻¹)	1.0	2.5	2.7
Maximum electron velocity(cms ⁻¹)	1 X 10 ⁷		1 X 10 ⁷
Electron mobility (cm ² (Vs) ⁻¹)	1500	400	2200
Hole mobility(cm ² (Vs) ⁻¹)	600	50	1600
Break down (X 10 ⁵ Vcm ⁻¹)	3	40	100
Dielectric constant	11.8	9.7	5.5
Resistivity (Ω cm)	10 ³	150	10 ¹³
Thermal conductivity (Wcm ⁻¹ K ⁻¹)	1.5	5	25
Absorption edge (μm)	1.4	0.4	0.2
Refractive index	3.5	2.65	2.42
Cohesive Energy (eV)	4.64	6.34	7.36

Table 1.3 (continued)

Young's Modulus (GPa)	130	450	1200
Shear Modulus (GPa)	80	149	577
Hardness(kg/mm ²)	1000	3500	10000
Fracture Toughness	1	5.2	5.3

1.2.4 Growth of Diamond

Two different growth mechanisms are in existence for growing diamond. One is the equilibrium growth at high pressure and the other being the metastable growth at subatomic pressures. The equilibrium growth of diamond can be carried out by a static or dynamic process. In a static process, the metastable graphite is dissolved into a liquid solvent and in a high-pressure press diamond precipitates as a stable phase whereas in a dynamic process graphite directly converts to diamond at high pressure and high temperature. Hydrocarbon gases are used for the metastable growth of diamond at sub atmospheric pressure. All the methods available for metastable growth of diamond differ in the means of generating hydrogen atoms.

1.2.5 Deposition Techniques

This section gives a brief overview of the popular deposition techniques for growing diamond films.

1.2.5.1 Hot Filament Assisted CVD

A tungsten filament placed above the substrate is heated at high temperature and a mixed gas of CH₄ diluted in H₂ is passed through the reactor for the growth of diamond films.

Unless the filament is hot, neither diamond nor the graphite can be deposited. The disadvantage is that the filament is carburized with the feed gas and thereby effects the growth of diamond. The atomic hydrogen helps the formation of single bonded carbon atoms and results in the formation of tetrahedral arrangement.

1.2.5.2 DC Plasma Assisted CVD

In this method, a DC bias is applied between the plate and the substrate. The plasma produced generates atomic hydrogen and carbon precursors for the growth of diamond. High nucleation densities of 10^8 cm^{-2} at a growth rate of $20 \mu/\text{hr}$ are possible. The advantage of this method is that no substrate pretreatment is required when diamond is grown on non-diamond substrates. However, the diamond films produced in DC plasmas were reported to have high stresses and contain high concentration of hydrogen and other impurities due to the plasma erosion of the electrodes. It was observed that when a positive bias is applied to the substrate and negative to the plate, diamond is deposited and in converse, graphitic carbon is produced when the applied bias is reversed.

1.2.5.3 RF Plasma Assisted CVD

The deposition is carried by inductive and plasma heating at a substrate temperature above 800°C . It was found that the high power in the discharge is necessary for efficient diamond growth. The grown diamond is found to have small grain size and good adhesion to the substrate. However, the high power results in the contamination forming SiC from the silicon crucible.

1.2.5.4 Microwave Plasma Assisted CVD

MPACVD is the popular technique for the development of diamond films. Surface wave sustained plasma excites the gas phase. The substrate is placed in the middle of the plasma and heated in the range of 800°C-1100°C by a heater. With this method, deposition is performed continuously from tens to hundreds of hours. The disadvantage of this system is that the quality of the film decreases with the increase in deposition rate.

1.2.5.5 Electron Cyclotron Resonance –MPACVD

In this method, the plasma is produced when the axial magnetic field due to the electromagnets has a value of 875 G (ECR condition). Electrons receive resonance impulses by preferentially absorbing the generated microwaves. The magnetic mirror confinement occurs at the ends of the plasma chamber and the ECR condition in the downstream. When the two electromagnets are placed close to the microwave window, ECR condition occurs within the plasma chamber. The drawbacks from most of these methods were the low growth rates, high temperatures and the difficulty in depositing on non diamond substrates. So the initial goals were to produce high quality diamond films on non diamond substrates at a higher growth rate and suitable temperature at which the growth of graphite would be inhibited.

1.2.6 Applications of Diamond Films and Coatings

- Optical coatings for the protection of softer materials against micro particle abrasion.

- Antireflection coatings for diamond optics.
- Oil-less diamond bearings are expected to have better performance than existing lubricated ones.
- Marine life does not attach to the diamond surfaces
- Diamond as a protective coating against salt-water corrosion.
- Diamond coatings can significantly reduce water drag and eliminate the need for liquid surfactants
- Semi conductor devices such as high frequency amplifiers, high power microwave devices due to its electron, hole mobility's, break down strengths, and reasonable band gap at high temperatures and relatively low leakage currents. Surface Acoustic Wave (SAW) applications due to high acoustic velocities.
- Diamond photodiodes
- Diamond field emitters due to its negative electron affinities (NEA's)
- Heat exchangers, condensers to furnaces due to high thermal conductivity
- Fabrication of high aspect ratio MEMS and NEMS components

1.3 Diamond-like Carbon (DLC) Films

Diamond-like carbon (DLC) films are amorphous in structure and has the properties almost comparable to that of diamond. The properties of these films predominantly depend on the deposition methods and process conditions employed. Even today, the nature of these materials is not understood to the full extent. These films are broadly classified as hydrogenated and non hydrogenated. The hydrogen content predominantly affects the structure of DLC films. Hydrogen content is less than 1% in non-hydrogenated

DLC films where as, it can be about 60% in hydrogenated DLC films. Usually, these films may have a combination of sp^3 , sp^2 and sometimes even sp^1 bonds.

Diamond-like hydrocarbons (a-C:H) are mostly deposited either by hydrocarbon ion beams or r.f. self bias plasma assisted CVD. The presence of hydrogen not only stabilizes the dangling bonds but also contributes in achieving wide optical gap and high electrical resistivity. The other major group is hydrogen free diamond-like carbon films popularly known as tetrahedral amorphous carbon as the films have a higher fraction of sp^3 bonds. The mass densities for these films vary from 1.4 to 2.0 g/cm³. DLC films usually have high compressive stress and the stress level increases with the increase in hydrogen content. The adhesive strength decreases with the increase in the hydrogen content. a-C:H films doped with Nitrogen have shown a reduction in compressive stress. DLC films have a smoother surface compared to diamond and hence have many applications that cannot be fulfilled by diamond films. Amorphous carbon (a-C) is deposited either by sputtering or by the pulsed laser ablation. PLD is the technique used for this research. The carbon plumes formed by laser vaporization are condensed on the substrate resulting in hydrogen free diamond-like carbon films. These films have carbon with greater mass densities and high hardness.

1.3.1 History of Diamond-like Carbon Films

Aisenberg and Chabot in 1971, first deposited diamond-like carbon films using carbon ions and these films had many properties of diamond. DLC are metastable and amorphous in nature. They can be deposited at temperatures less than 325°C [25]. Kaplan et al in 1985 found that hydrogenated DLC films, depending on the deposition method,

contains hydrogen varying from 10% to 60%. In 1986, Robertson reported that even though DLC lack long-range order they possess short or medium range order [11]. In 1971, Aisenberg and Chabot succeeded in depositing hydrogen free DLC films using C⁺ ions in Argon environment.

1.3.2 Structure of Diamond-like Carbon Films

The structure of DLC consists of both three fold coordinated sp² and four fold coordinated sp³. While the sp² controls the electrical properties like band gap, sp³ controls the mechanical properties like hardness and rigidity of the film. The four fold coordinated sp³ is the characteristic of hard diamond. The four valence electrons of carbon atom are tetrahedrally bonded to each other forming the strong σ bond. The three folded sp² carbon atom is the characteristic of graphite. In graphite, the three valence electrons of carbon atom form a strong σ bond and the fourth atom forms a weak and unsaturated π bond normal to the σ bond.

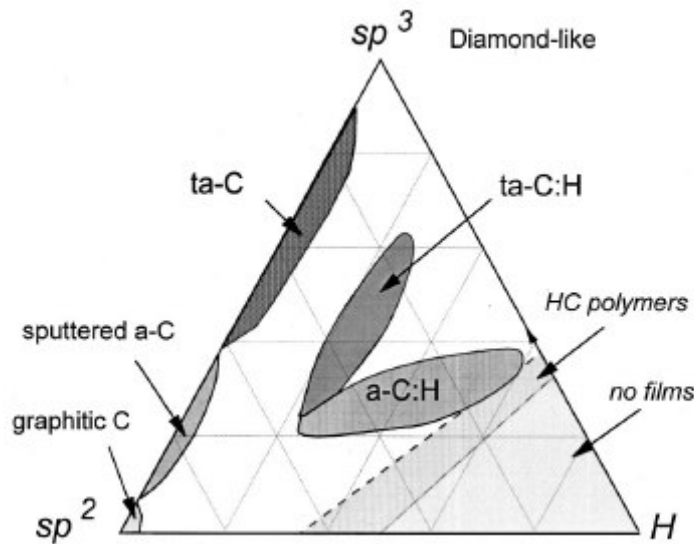


Figure 1.2 Ternary Phase Diagram of DLC Films Showing sp^3 , sp^2 , and H Contents[8]

Figure 1.2 represents the compositions of DLC films with respect to sp^3 , sp^2 and H contents. From the phase diagram, it can be concluded that the hydrogenated amorphous carbon films has less percent of sp^3 bonds. The ta-C has the highest sp^3 fraction. Even though the films have same sp^3 and hydrogen content, the properties of the film vary depending on the sp^2 clusters in the film. Sputtered amorphous carbon films have more of sp^2 content. The a-C:H films are located at the center of the phase diagram and has varying amounts of sp^3 , sp^2 and H contents. With the increase in the hydrogen content, sp^3 content decreases and the optical transmission and band gap increases.

1.3.3 Mechanical Properties

The mechanical properties like hardness, friction, wear resistance and elasticity depend mainly on the strength of the sp^3 bond. The presence of hydrogen does not affect the elastic property of the film. It mostly depends on the sp^3 and sp^2 content. This property is the measure of resistance to deformation. The intrinsic stresses in the film also determine

the quality of the film. The intrinsic stresses limit the maximum thickness of the DLC films that in turn limits its use in applications demanding the thick coatings. It has been shown that the stresses in the film can be reduced by reducing the sp^3 content in the film [9]. The sp^3 bonds usually strain the links resulting in high compressive stresses. Dekempeneer et.al. observed the decrease in the stress with the change in bias voltage from -200V to -400V [10]. Most of the important applications of DLC can be attributed to its friction and wear properties combined with its hardness. Pin on disk is the most popular method used for measuring the coefficient of friction.

1.3.4 Deposition Techniques

Diamond-like carbon films are divided into two main sections. One being the hydrogenated and the other is non-hydrogenated DLC. Numerous techniques are available to deposit diamond-like carbon films. But not all the techniques can produce hydrogen free a-C coatings. In this section, different deposition techniques available for depositing hydrogen free a-C thin films are discussed.

1.3.4.1 Filtered Cathodic Arc Deposition

This is the best technique to produce hard tetrahedral amorphous carbon thin films. The apparatus is equipped with a magnetic filtering technique that efficiently removes the macro particles and hence improves the smoothness of DLC film even at the room temperature. Graphite is used as the cathode source and carbon ions are produced in vacuum, between the graphite cathode and anode. The arc currents used are in the range

of 40 – 90 A. A bias voltage of 100 to 300V is applied to control the ion energy at the substrate. The sp^3 content in these films is very high and thus the films exhibit high hardness compared to the films deposited by other techniques.

1.3.4.2 Pulsed Laser Deposition

Pulsed laser ablation is considered as the best technique for the deposition of hydrogen free diamond-like carbons. The sp^3 content is high in PLD deposited films because the laser energy transforms the sp^2 bonds to sp^3 bonds. The shortwave length of the excimer laser results in the deposition of atomically smooth surface of the films.

1.3.4.3 Magnetron Sputtering

N.H Cho et al, reported the change in structure and physical properties of sputter deposited amorphous carbon with the change in the power density. They showed that graphitic features increase with the increase in the power density. Hydrogen free DLC can be deposited by sputtering a carbon target in the presence of Argon gas. Even hydrogenated diamond can also be deposited using a mixture of Argon and Hydrogen gas while sputtering. Paik [12] showed that the amount of sp^3 bonds in the film depends on the ion energy. It was observed that the sp^3 content increased with the increase in the ion energy. The pyrolytic graphite target is sputtered in the presence of Argon gas to get the amorphous diamond-like carbon films. Hydrogenated DLC can also be prepared by passing a suitable hydrogen precursor gas.

1.3.5 Applications

Because of the low friction, high wear resistance and reasonable hardness DLC films have many applications. Few of them are listed below:

- DLC is used as protective coatings from razor blades to magnetic tapes. With its self-lubricating property, DLC facilitates the motion of hard disk beneath a floating head.
- DLC is used as anti reflecting coating for Silicon solar cells.
- High hardness combined with a low coefficient of friction makes DLC the best material for MEMS applications
- DLC coated cutting tools exhibited an increased lifetime.
- Biocompatible material for orthopedic implants.
- Cold cathode field emitters
- Anti-scratch coatings for optical applications, infrared optics, sunglasses, optical Lenses.
- IR sensors and lenses.
- Optical and electronic components.

1.4 Literature Review

Diamond and diamond-like carbon coatings has been the topic of interest to the researchers because of its excellent mechanical, tribological and optical properties. But unfortunately, the high compressive stress of these films demotes its numerous applications. Due to the formation of sp^3 bonds, the compressive stresses are more in these films and hence have the poor adhesion. Stresses in the films can be relieved by

carrying out the deposition at high substrate temperature. Unlike diamond, which is stable even at high temperatures, DLC graphitizes at a temperature near to 400°C. To overcome these problems many researchers have succeeded in developing metal-doped DLC films. These films have showed better adhesion and improved wear properties. TiC and WC were successfully incorporated in DLC films and improvement in the film properties has been obtained [1].

A.A.Voevidin et.al. [2] designed a stack of multilayered interlayers with different ceramics and soft metals to improve the adhesion of DLC films on stainless steel substrate. The layers of the selected materials were deposited in such a way that the modulus increases from bottom to the top layer. A combination of magnetron sputtering and PLD were used to deposit functionally gradient metal/ carbide/ DLC coatings. The use of ductile Ti interlayer increased the coating scratch resistance, Ti and TiC interlayers enhanced the friction coefficient and the wear rates, compared to the single layered DLC films.

C.Donnet et.al. [3], conducted experiments to study the relationship between the deposition conditions and the film composition, the properties like stress, and friction of the interlayered DLC films. Ti/a-C:H films were deposited using a hybrid technique of magnetron sputtering and d.c plasma enhanced chemical vapor deposition with the bias voltage between -35V to -260V to optimize the deposition conditions exhibiting ultra low friction in ultra high vacuum. The investigation revealed that depending on deposition conditions, DLC films exhibit a wide range of friction behavior, the lowest coefficient of friction being exhibited by the films deposited at lowest bias.

Mosaner et.al. [4] succeeded in reducing the internal stresses in DLC films by thermal annealing. The films deposited using PLD were annealed in air to study the effect of annealing temperature and time on the reduction of stresses in the films. By thermal annealing, they deposited films that are more than one micron thick with comparatively low stresses as the internal stresses are relieved due to relaxation of chemical bonds in the film.

Sood et.al. [5], first investigated the growth of diamond film on Ti-6Al-4V, by varying the dose of carbons ions implanted into the samples at room temperature. The deposition of diamond was carried out by microwave chemical vapor deposition at a substrate temperature of 1000°C. With the increase in the ion dose, a reduction in the nucleation density was reported. The Raman spectra revealed the presence of diamond particles, and the films were peeled off due to the presence of high internal stress.

Fu et.al. [6], studied the effect of deposition conditions on the stresses developed in the diamond films on a Ti substrate. The compressive residual stresses increased with the increase in the deposition time, high concentrations of CH₄ also increased the stresses, and this resulted in the delamination of the films. They proposed the method of using interlayers to reduce the stresses and observed that the presence of nitride layer decreased the compressive stresses to a significant extent and improved the adhesion of the diamond films on Ti alloys.

1.5 Overview of the Thesis

Diamond and diamond related coatings have superlative mechanical, thermal, optical and electronic properties. These coatings demonstrate high chemical inertness to almost all

the environments. The major concern associated with these films is that they suffer from high compressive stresses that cause the delamination of the films and this is the main drawback of diamond and diamond related materials that reduce their applications.

Development of stresses in thin films is due to temperature changes, lattice mismatch, high energy of deposited ions and implantation of foreign atoms in the deposited films. Intrinsic stresses are developed during the growth of thin films. As the thickness of the films increase, the stresses increase causing the failure of the films by cracking, buckling and delamination even before the wear. Films with compressive stresses are more desirable compared to tensile stresses as the former increases the strength whereas the latter causes cracks in the films. Stresses due to lattice mismatch can be avoided by using nitride and carbide interlayers. The other factor influencing the quality of films is the adhesive strength at the interface. For thin films, the stresses and the adhesion between the substrate and the film are interrelated. Improvement in the adhesion energy paves path for the prevention of buckling and delamination caused due to high stresses. Even the coefficient of friction of films decreases with the decrease in the stresses.

The present research focuses on the reduction in the stresses for both diamond and diamond-like carbon (DLC) films using different materials as interlayers. Micro Raman spectroscopy is used to find the structure and also the stresses in the films. The mechanical properties and the coefficient of friction are evaluated using the Nanoindenter XP and the ball on disk method respectively.

CHAPTER 2
EXPERIMENTAL TECHNIQUES

Diamond and diamond-like carbon coatings are primarily deposited using vapor deposition techniques like chemical vapor deposition (CVD) and physical vapor deposition (PVD). Though both are atomistic deposition techniques, deposition in CVD is because of chemical reaction, and in PVD deposition is due to condensation.

Table 2.1 Properties of Diamond and DLC Materials

Property	Thin Film		Bulk		
	CVD Diamond	a-C	a-C:H	Diamond	Graphite
Crystal Structure	Cubic $a_0=3.561$ Å°	Amorphous mixed sp^2 and sp^3 bonds	Amorphous sp^3/sp^2	Cubic $a_0=3.567$ Å°	Hexagonal $a=2.47$ Å°
Form	Faceted crystals	Smooth or rough	Smooth	Faceted crystals	
Hardness (H_v)	3000- 12000	1200-3000	900-3000	7000- 10000	
Density (g/cm^3)	2.8-3.5	1.6-2.2	1.2-2.6	3.51	2.26
Refractive Index	-	1.5-3.1	1.6-3.1	2.42	2.15
Electrical Resistivity (Ω/cm)	$>10^{13}$	$>10^{10}$	10^6-10^{14}	$>10^{16}$	0.4
Thermal Conductivity (W/m.K)	1100	-	-	2000	3500
Chemical Stability	Inert	Inert	Inert	Inert	Inert
Hydrogen Content (H/C)	-	-	0.25-1	-	-
Growth Rate ($\mu m/hr$)	~1	2	5	1000 (synthetic)	-

This chapter gives a brief overview of the different techniques used for the deposition of diamond related materials. PLD and MPCVD techniques are used for diamond-like carbon and diamond respectively. Table 2.1 gives the properties of diamond and DLC materials.

2.1 Diamond-like Carbon Films

2.1.1 Pulsed Laser Ablation

Pulsed laser ablation is one of the most renowned techniques for thin film deposition. Thin film is formed by the condensation of the ablated target material, with or without the background gas, on the surface of the substrate. J.Cheung is the first one to come up with the numerous advantages of Pulsed Laser Deposition. Since then PLD is used for the deposition of different materials like ferroelectrics, metals, high temperature superconducting thin films and ceramics. The main advantage of PLD is its ability to deposit materials containing more than 5 to 6 compounds without changing the stoichiometry of the material that is otherwise difficult to achieve with other available methods. Other advantages include the deposition of multilayered epitaxial films with the aid of target carousel, deposition in vacuum, inert or reactive gases and high energies of the ablated species.

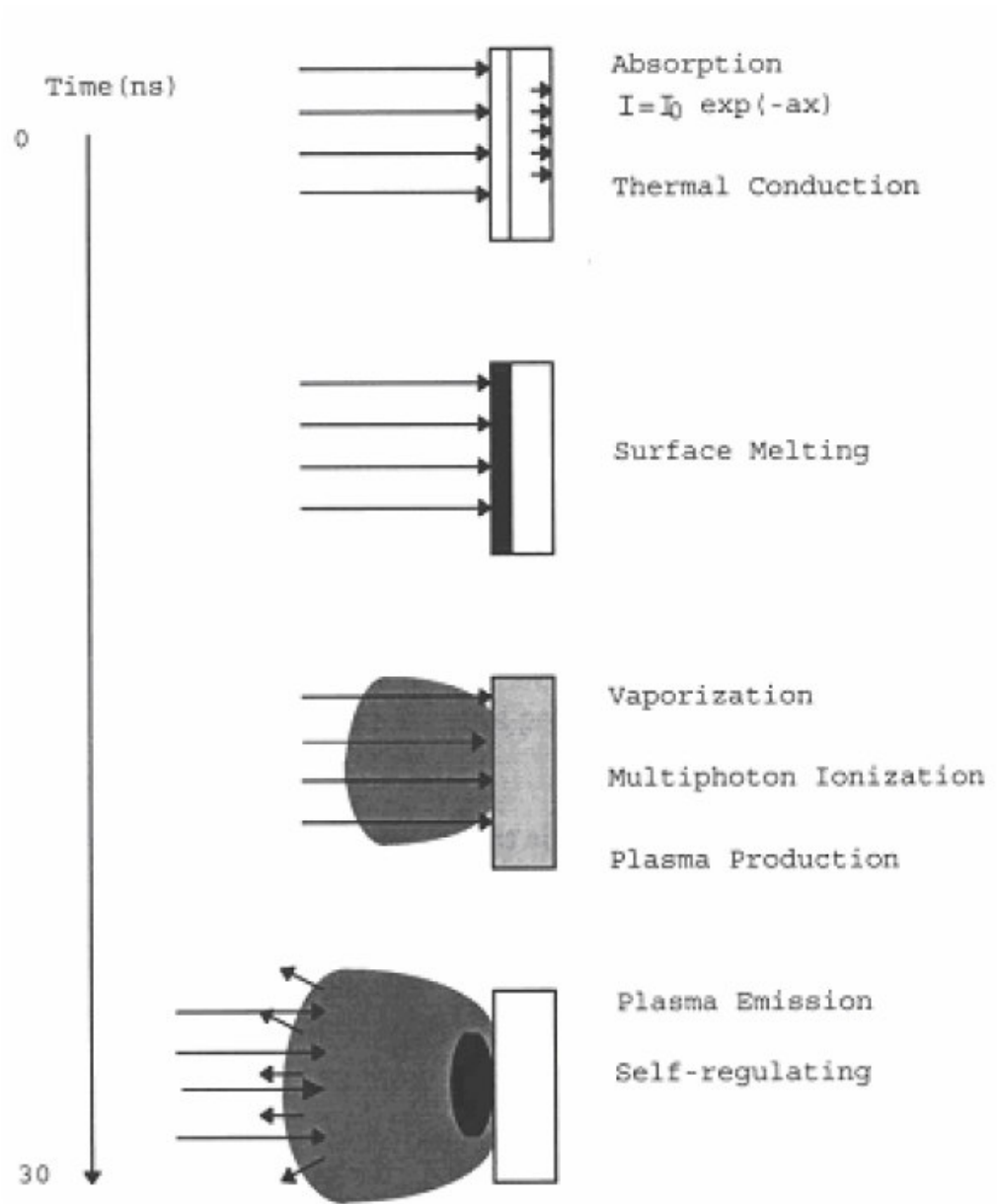


Figure 2.1 Schematic Representation of Laser-Target Interactions [13]

Though PLD is simple to operate, it is difficult to understand the ablation process because of the complexity involved in the laser beam solid interaction. Figure 2.1 shows the schematic of laser target interactions. There are many proposed models, the details are given elsewhere [13]. No single model discusses the effect of all the aspects on the

laser solid interactions as models are developed taking a particular feature into account and neglecting the others. It can be better explained as a two step process 1) heating of the material surface with the absorption of photons and 2) formation of the molten layer that vaporizes. The target material is irradiated by the laser energy. The electromagnetic radiation absorbed by the solid surface is converted to electronic excitation and then to thermal, chemical and mechanical energy, which in turn, causes evaporation, ablation, excitation and plasma formation.

The main drawback associated with the PLD is the formation of micron sized particulates on the films. They are deposited because of the target inhomogenities, fluctuations in the laser energy and so on. Mainly three approaches have been developed to reduce these particulates. Particulates can be controlled by reducing the laser energy fluctuations and inhomegenities in the target [14]. The other approach is the use of velocity filter that ejects the massive particles with relatively smaller velocities than those of atomic and molecular species [15]. Third one being the off axis deposition in which the substrate is placed parallel to the laser plume [16]. The other concerns are poor film reproducibility, non uniformity of thickness when deposited over large areas.

PLD has emerged as one of the most competent technique for depositing hydrogen free amorphous carbon thin films. Extensive research has been done to study the effect of laser density, substrate temperature [17] on the properties of diamond-like carbon thin films. Depending on the laser density and the substrate temperature, the optical and electrical properties can be tailored between diamond and graphite [17]. The main

advantage of pulsed laser ablation over CVD is that the deposition temperature can be low as the kinetic energy of the depositing species is very high. CVD is preferred if the substrate can withstand the high temperature.

The PLD system at USF uses the KrF excimer laser, the most popular for pulsed laser ablation. It has a wavelength of 248 nm with photon energy of 5eV. The system has a laser generating unit, vacuum chamber, optical elements to focus the laser beam on to the target, target carousel that can hold four target holders and substrate holder, mass flow controllers, vacuum pump and a substrate heater that can go to a maximum temperature of 650°C. The chamber is equipped with two rotary feed through, one of which allows selecting the required target for the deposition.

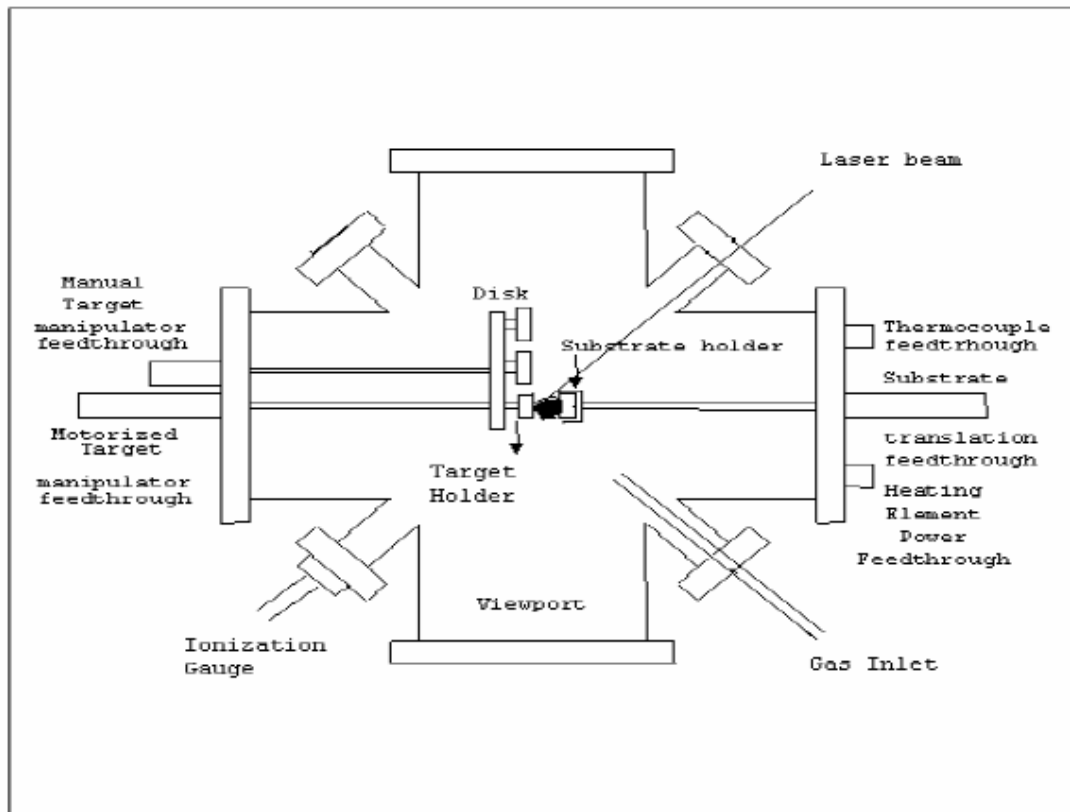


Figure 2.2 PLD System at USF

The other being the target rotator that helps to avoid the crater formation due to prolonged exposure to laser at a particular position of the target. Films can be deposited in Ultra high vacuum, the order of 10^{-7} torr. Figure 2.2 shows the schematic of the PLD system at USF.

2.1.2 Experimental Procedure

Lambda Physik KrF excimer laser was used for the deposition of diamond-like carbon films and the interfacial films. The PLD system contains target holder that can accommodate four different targets at a time. This feature can be used to deposit multilayers without breaking the vacuum. The deposition chamber was evacuated to millitorr range using a mechanical pump and then high vacuum is created using the turbo molecular pump. All the depositions were carried out in a pressure range of 10^{-7} Torr. High power UV optics were used to focus the laser on the target at a pulse rate of 10 Hz and the laser energy is fixed at 300 mJ.

The substrate, Si(100) is cleaned ultrasonically in methanol and acetone. Pyrolytic graphite (99% purity) is used for the deposition of ta-C films that are deposited at different temperatures, room temperature (RT), 100°C, 200°C, 300°C, 400°C on Si(100) substrates, respectively. The substrate to target distance was maintained at 4 cm for all the depositions.

Interlayered DLC were deposited with the aid of multiple target holder. The desired targets were mounted on to the holder prior to the experiment and were rotated to bring the required target under the laser irradiation. In this research TiC, TiN, AlN, TaN, W and Ta were used as the interlayers and their effect on the performance of DLC films was

investigated. The interlayers are deposited at 100°C, 300°C and 600°C whereas the ta-C is deposited at 100°C for all the experiments.

2.2 Diamond Films

It is difficult to grow a diamond that is free of defects. The physical properties of diamond are greatly affected by the presence of defects like point defects, dislocations and stacking faults. Diamond lattice has boron, nitrogen, hydrogen and oxygen as substitutional defects. Presence of Nitrogen leads to less thermal conductivity [18]. With the increase of nitrogen concentration diamond becomes colorless and also it affects the different material properties. For HPHT the growth rates should be as low as possible to reduce the defects and it is difficult to maintain the required conditions for a long time. The flexibility of varying the conditions makes the CVD technique a better option compared to HPHT. Hence, diamonds with fewer defects can be efficiently produced using the CVD method.

2.2.1 CVD Deposition Technique

The deposition of diamond was initially carried by methods such as ion beam method, ion implantation, and chemical vapor deposition techniques (CVD). Of these methods, CVD process has drawn much attention as the films can be grown on any dimensional scale, shape and thickness. CVD of diamond from hydrogen rich hydrocarbon containing gases has been the most successful method. In this process, the plasma ball is produced inside the reactor (deposition chamber) very near to the heated substrate by applying high power and disassociating the feed gases (Hydrogen and Hydrocarbon species (CH_4)) into free radicals such as CH_3 , CH_2 , and CH . These excited hydrocarbons generate carbon

atoms and some of these excited carbon atoms deposit as a diamond film while others decay their energy during their migration and deposit as graphitic carbons or non diamond carbons. In presence of hydrogen, a chain reaction converting the non diamond carbons to hydrocarbons take place and again produces the diamond species. The growth of diamond is ensued as long as this chain reaction continues. At the same time, a spontaneous graphitization takes place. It is necessary to inhibit the nucleation of graphite while adding the carbon atoms to the surface. Hence, most of the growth processes involve termination of diamond surface with hydrogen or a halogen since both hydrogen and halogen can form a high energy bond with carbon than the carbon atom itself.

The advantages of hydrogen or halogen termination are listed below:

- 1) To prevent the formation of any unwanted C-C π bonding on the diamond surface and thereby preventing the growth of graphitic species.
- 2) The partial pressure of the carbon atoms in the vapor phase is so low that the free atoms are not probably the major source of carbon for the growth of diamond. More likely, a reaction of CH₄ or other hydrocarbon with the diamond surface might result in the deposition of a carbon atom.
- 3) Prevents the rapid growth at nominal temperatures. As the growth temperature is increased to a certain extent, smaller amount of the surface is terminated and provides a larger number of denude sites for arriving carbon atoms to form a tetrahedral bond.

There are other methods such as addition of oxygen surfactants, which have less bond energy than C-C so that the arriving carbon atoms can replace these surfactant atoms. However, the molecular hydrogen alone is not sufficient to completely suppress the growth of graphite. Hence, atomic hydrogen is used to remove the same. Also, in case of conventional hydrogen termination, only one in every 10^4 hydrogen atoms is replaced by a carbon atom.

The growth of diamond in a metastable region would be possible if the following conditions are satisfied.

- 1) Formation of mobile species containing a single carbon atom by collision of CH_4 with diamond surface.
- 2) Rapid diffusion of carbon containing surface species
- 3) Formation of diamond by addition of carbon surface species to a vacant site.

The difficulty in the diamond synthesis was due to extremely short life time of the excited carbon atoms. The life time of the carbon atoms can be increased either by incorporating atomic hydrogen species, by disassociating a carbonaceous compound, electric discharge, electron bombardment, UV irradiation, shocks and shears, x-rays. The growth of CVD diamond has been introduced; different methods existing and their time line is listed in Table 2.2.

Table 2.2 History of CVD Diamond

Method employed	Year
HFCVD	1981
MPCVD and RFCVD	1982
Electron assisted CVD	1982,1985,1987
DC plasma CVD	1982
RF thermal plasma CVD	1987
DC plasma jet CVD	1988
Arc Discharge plasma CVD	1988,1989
Magneto microwave plasma CVD	1987

2.2.1.1 Microwave Plasma Assisted CVD

MPACVD is an electrode less process and thereby prevents the contamination of the films due to the electrode erosion. Due to the short wavelength or high frequency generator (12.4 GHz), higher plasma density is produced and the growth of diamond is enhanced when compared to a low frequency HF-CVD method (13.6 KHz). A very intensive localized discharge is obtained with a little tendency to spread. It is suitable for producing atomic hydrogen, nitrogen and oxygen. The plasma generated by microwave is stable for a long time.

$$E_{\max} = (QE)^2 / 8\pi^2 f^2 M$$

E_{\max} = maximum ion energy

Q = Ion charge

M = mass of ion

f = frequency

The maximum energy has to be small so that the ions produced will not etch the diamond surface. The disadvantage is the strong tendency to deposit the isolated particles on the non diamond substrates.

2.2.2 Experimental Procedure

The interlayer coatings such as TiN and TiC, were deposited using PLD as it combines the advantage of stoichiometric deposition at lower temperatures with little contamination. Prior to the deposition, the substrates were cleaned using acetone and methanol and were loaded in to the vacuum chamber. Using a turbomolecular pump, the chamber is evacuated to a base pressure of 10^{-7} Torr. Both the interlayers are deposited at a substrate temperature of 300°C.

The samples with interlayers are treated in diamond particle suspension for 25 minutes using an ultrasonic bath and then cleaned in methanol. The substrate was then loaded in to the MPCVD chamber and the deposition was carried out in the presence of methane and hydrogen at a temperature of 800°C.

CHAPTER 3

STRUCTURAL AND MECHANICAL CHARACTERIZATION

Characterization describes those features of composition and structure (including defects) of a material that are significant for particular preparation, study of properties, or use, and suffice for reproduction of the materials. This chapter reviews the techniques used to characterize the diamond and diamond-like carbon coatings.

3.1 Raman Spectroscopy

Raman spectroscopy has emerged as a powerful technique to identify the molecules and study their structural properties. It is based on the fact that the molecules interact with the electromagnetic field of the incident radiation and vibrate at characteristic frequencies of those materials. In 1928, Chandrasekhara Venkata Raman discovered the phenomenon of Raman Effect. It is a simple phenomenon, where the monochromatic light is focused on the sample and the scattered light is analyzed for the required information.

Raman spectra are observed in the UV-visible region and is concerned with the vibrational transitions that appear in the 10^4 to 10^2 cm^{-1} region. The spectrum consists of Rayleigh scattering that has same frequency as the incident radiation and a weak line corresponding to the Raman scattering that has a shift in frequency. Depending on the

increase or decrease in the frequencies, the lines are called stokes and anti stokes, respectively. Usually Raman spectra are observed for the vibrational and rotational transition. A transition is said to be infrared active if there is a change in the dipole moment of the molecule and is Raman active if there is a change in polarizability of the molecule.

The commercially available Raman spectrometer has five main components. Continuous wave laser like Ar⁺ at a wavelength of 514.5 nm are used as excitation source. Sample illumination and scattered light collection system, sample holder, monochromator or spectrograph and detection system are the other important components in the Raman spectrometer. Laser is focused on the sample placed under the microscope that excites the sample and the scattered light is collected in the same path as the incoming laser. The scattered light is dispersed on to a charge coupled device (CCD) detector. The sample size needed for Raman spectroscopy is small as the focused laser beam is 1-2 mm in diameter. The disadvantage of Raman is that it needs a powerful laser source to observe weak Raman scattering.

Applications: Raman spectroscopy is widely used in chemistry as this technique depends on the vibrational transitions that are specific to the chemical bonds. It has many applications like real time monitoring of anesthetic and respiratory gas mixtures at the time of surgery.

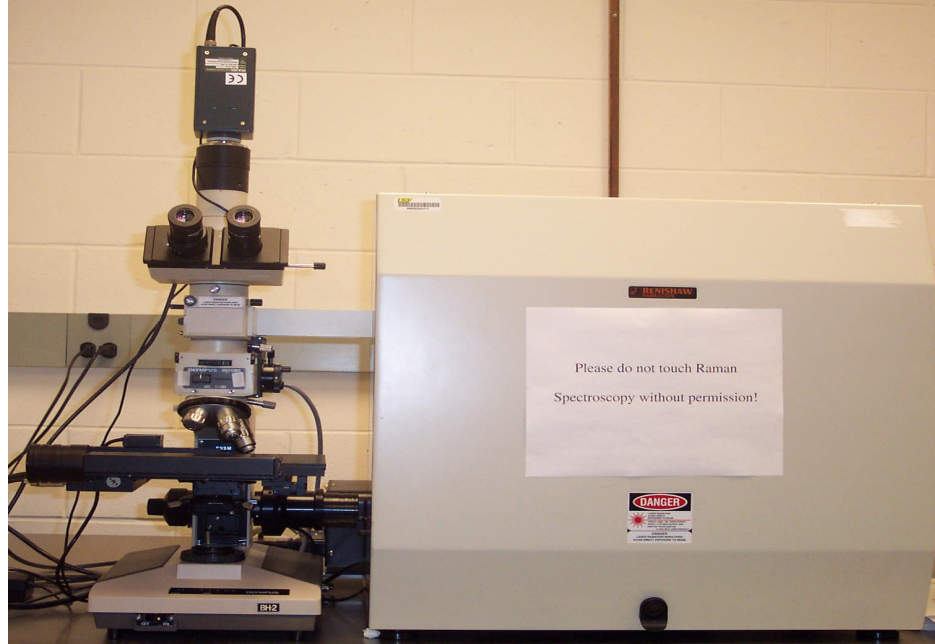


Figure 3.1 Renishaw Raman Spectrometer at USF

3.2 Nanoindentation

The mechanical behavior of thin films at micro level or less cannot be deduced from the properties of the bulk materials. Even the behavior is not same for a free standing film and the one attached to a substrate. This can be mainly attributed to the change in the microstructure, dislocation density and vacancy concentration differences. Nanoindentation is one of the popular techniques for measuring the mechanical properties of thin films. In this method, an indenter is driven into the material and the applied load and displacement are continuously monitored. Recently, different depth sensing indentation instruments have been developed for performing the nanoindentation. With these instruments, it is possible to make shallow indentations at the required locations. There are many proposed methods to analyze the data obtained from these

instruments [19] and issues to be considered in the analysis of data and are discussed briefly by Cripps [20].

In nanoindentation a hard indenter, typically made from diamond, with known tip geometry is driven into the material to be tested by increasing normal load. When a preset maximum value is reached, the load is reduced until partial or complete relaxation. The residual impression is measured and the hardness is defined as the ratio of maximum load, P , to the residual area A_r .

$$H = \frac{P}{A_r}$$

Now, the problem is finding the indentation area. Direct measurement of the residual area of a small indent is difficult. To solve this problem depth sensing indentation method was developed. In this method, at each stage of the experiment the position of the indenter relative to the sample surface is precisely monitored with a sensor. The obtained data is analyzed to find the contact area without having to measure the residual impression manually. Figure 3.2 shows the typical load vs displacement plot for obtained data.

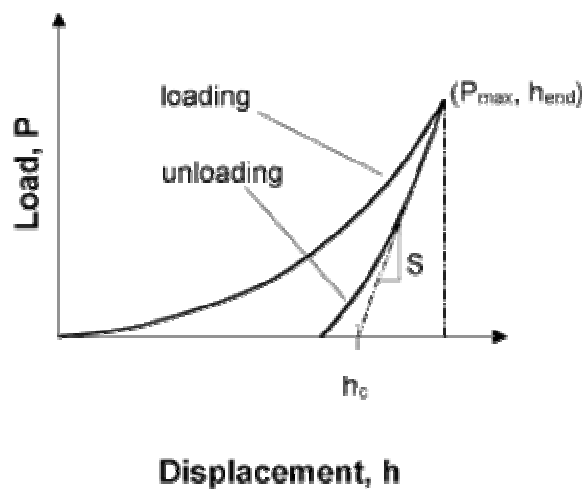


Figure 3.2 Plot of Load vs Displacement Data

3.3 Nanoindentation Data Analysis

Once the load-displacement data is collected, there are different proposed methods to analyze the data and obtain mechanical properties.

3.3.1 Doerner and Nix Method

This method states that if the change in the contact area is small during unloading, the indenter can be treated as a flat punch. They assumed that all the material in contact with the indenter is plastically deformed and obtained equations to find the contact area from load displacement data [20].

3.3.2 Oliver and Pharr Method

This method predicts that the unloading data for an elastic contact for different indenter tip follows a power law that is given as,

$$P = \alpha h^m$$

where ,P, is the indenter load , h is the elastic displacement, and α and m are constants.

3.3.3 Basic Equations Involved

There are set of governing equations available to calculate the hardness and modulus values from the given load vs displacement data. The Nanoindentation equipment works on the basis of these classic equations. To find the hardness, the contact area at maximum load is used. If the shape of the indenter tip is accurately known, a tip area function can be generated.

$$A_c = f(h_c)$$

h_c is the contact depth ,where the indenter is in actual contact with the sample.

The hardness is now given as,

$$H = \frac{P_{\max}}{A_c}$$

The slope of the initial unloading gives the contact stiffness,

$$S = \frac{dP}{dh} = \frac{2\sqrt{A}}{\sqrt{\pi}} E_r ,$$

where E_r is the combined modulus or the reduced modulus that combines the modulus of indenter and the specimen and is given by

$$\frac{1}{E_r} = \frac{(1-\nu_i^2)}{E_i} + \frac{(1-\nu_s^2)}{E_s}$$

where i , corresponds to indenter and s , to the sample .

The tip used during this research is a berkovich tip. The analysis of test data for a berkovich indenter is discussed here. The berkovich indenter has an included half angle of 65.3°. The relationship between the projected area, A , of the indentation and the actual depth of contact, h_p , is given as

$$A = 3\sqrt{3}h_p^2 \tan^2 65.3 = 24.5h_p^2$$

Once ' h_p ' is calculated, the hardness is obtained using projected contact area.

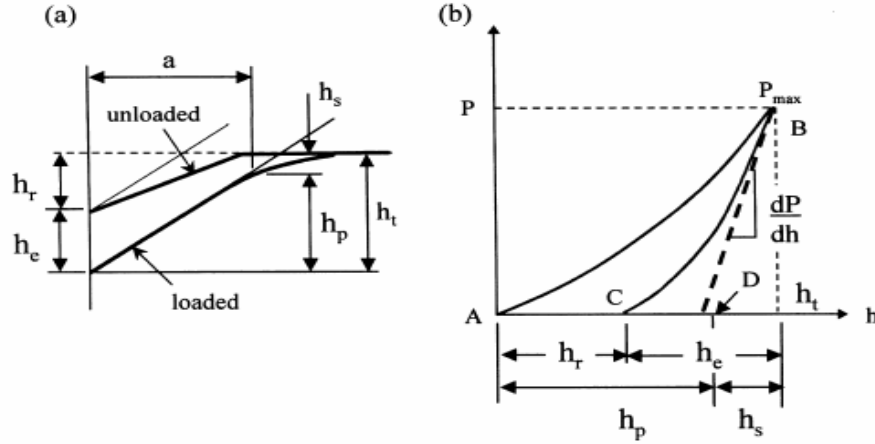


**Figure 3.3 a) Schematic of Indenter and Specimen Geometry
b) Load Displacement Curve**

h_e = is the elastic deformation of the specimen

h_p = the actual contact depth

h_r = is the depth of contact beneath the specimen free surface

h_t = is the total penetration depth

In order to reduce the complexity involved in the numerical calculations, berkovich indenter is considered as a cone with a semi angle of 70.3° that gives the same area to depth ratio.

For completely elastic contact, the relationship between the load and the depth of penetration for a cone is given by

$$P = \frac{2E^* \tan \alpha}{\pi} h^2$$

The derivative of the above equation gives the slope, i.e., stiffness as

$$S = \frac{dP}{dh} = 2 \frac{2E^* \tan \alpha}{\pi} h$$

With the appropriate substitutions for h , the elastic modulus for the specimen tested using a berkovich diamond indenter is given as

$$E^* = \frac{dP}{dh} \frac{1}{2h_p} \frac{1}{\beta} \sqrt{\pi/24.5}$$

Nanoindentation is performed for all the samples and the results are discussed in the fore coming chapter. Figure 3.4 shows the schematic of the nanoindenter XP used for this research.

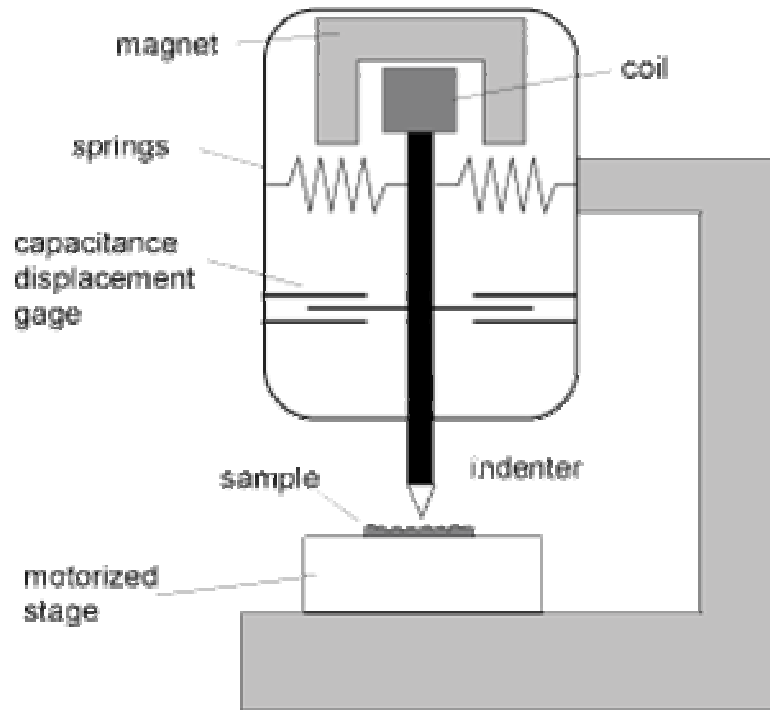


Figure 3.4 Schematic of Nanoindenter XP

3.4 X-Ray Diffraction

Each of the elements existing has different properties like structural, physical, mechanical, thermal and electrical, etc. These properties have to be studied to better understand how different elements can have their applications. Different analytical tools

have been invented to study the structural, physical, morphological, optical and electrical properties etc. Of these, the study of structural properties becomes important as they largely determine the remaining properties of the materials. One of the important techniques used to study the structural properties is XRD (X-Ray Diffractometer).

The atomic planes of a crystal cause an incident beam of X-rays (if wavelength is approximately the magnitude of the interatomic distance) to interfere with one another as they leave the crystal. The phenomenon is called X-ray diffraction [21]. As an x-ray beam travels through any substance, its intensity decreases with the distance traveled through the substance. Only a small range of characteristic x-rays are widely used for diffraction. When the voltage on an x-ray tube is increased above a certain value then the wavelengths of characteristic lines of target metal are obtained. These characteristic lines are denoted by K_{α} , K_{β} and K_{γ} . These characteristic lines were discovered by W.H.Bragg. He and his son W.L.Bragg have done a foremost experimentation of finding out the crystal structures of NaCl, KCl and KBr etc. The famous Braggs law was formulated based on which the diffraction studies are carried out.

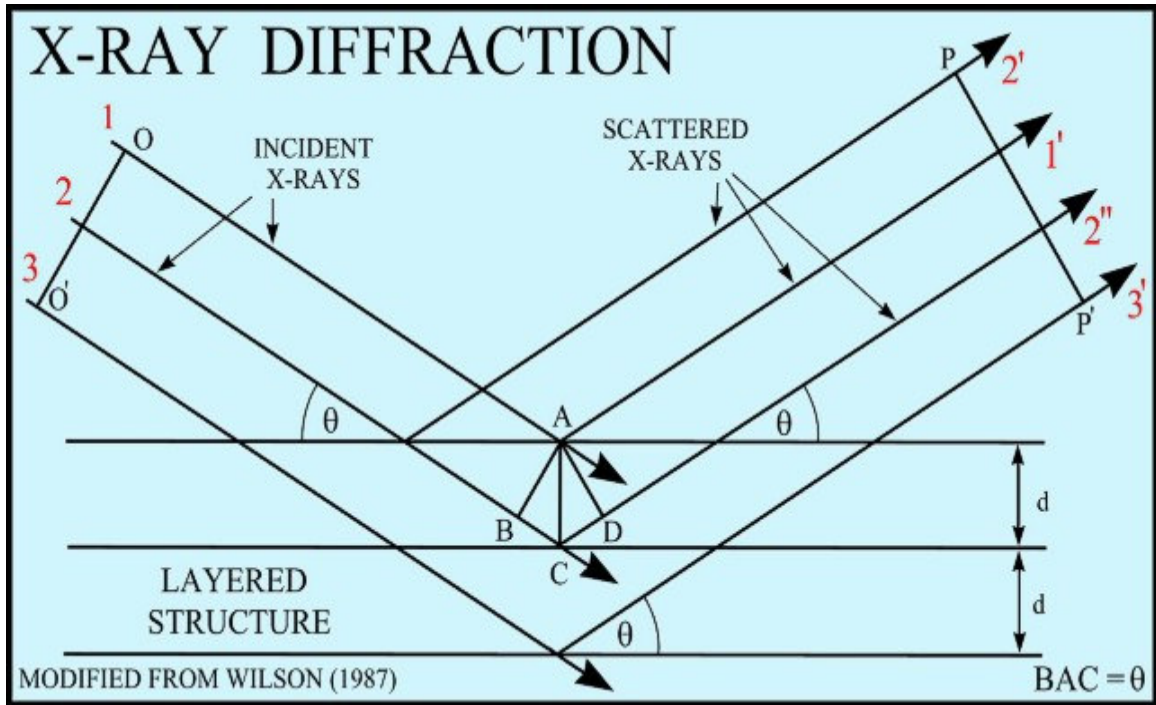


Figure 3.5 X-Ray Diffraction [26]

$$n\lambda = 2d(\sin \theta)$$

n = order of diffraction

λ =wavelength

d = separation between the planes

θ =angle of incidence beam

3.5 Friction Test

Universal Micro Tribometer (UMT), a tribological testing apparatus, is used for the friction test of the specimen samples. The apparatus, which has load sensor and feed back control from a PC, is operated using the software controls on the PC. Machine can be operated according to several test procedures that can be programmed as sequences, which in turn can be edited and are very flexible. It eliminates the need to program the whole procedure again for low cycle tests. The X and Z direction forces and

displacements are measured using the load sensor and the software automatically plots all the values of the coefficient of friction, force due to friction in the X direction and force (applied) in Z direction. Static and sliding coefficient of friction can be obtained from the graph.



Figure 3.6 Universal Micro Tribometer with PC Based Feed Back Control

3.5.1 Description of UMT

Main features of the universal micro tribometer are as follows:

- 2D force sensor to measure the friction and normal load with a force range of 1-100 N or 0.22 – 22 lb with a resolution of 0.1 N or 0.022 lb.
- PC based 12-channel data acquisition and 3 motor controllers.

- Testing block, which is made of high-density cast iron vibration damped frame.
- Upper vertical positional system has 150 mm of travel at 0.001-10 mm s⁻¹ with 1 micron resolution.
- Upper lateral positioning system has 75 mm of travel at 0.01-10 mm s⁻¹ with 2 micron resolution.
- Tribometer is facilitated with load feed back control system and suspension for the force sensor.
- Automatic sequencing of tests and data acquisition
- Additional sensors like the contact acoustic emission detector and electrical contact resistance.

CHAPTER 4

RESULTS AND DISCUSSION

4.1 Amorphous Carbon Films without Interlayer

The mechanical properties of silicon, which is an important material in electronic packaging, are improved with a amorphous carbon (a:C) coating. Owing to the compressive stresses in the film, the a:C exhibits a poor adhesion with the silicon. This work focuses on the use of carbide and nitride interlayer to improve the adhesion between silicon and a:C by reducing the stresses. Amorphous carbon was deposited on Silicon substrate using the PLD method as discussed in section 2.1.2. The structural and the mechanical properties of the a-C films were studied as a function of deposition temperature. The structural properties of the films were characterized by the Raman spectroscopy and the mechanical properties by nanoindentation and friction test. This section presents the results and discussion of the tetrahedral amorphous carbon without any interlayer. All the films were deposited at five different temperatures – Room Temperature (25°C), 100°C, 200°C, 300°C, and 400°C.

Using an optical microscope, it was observed that the films buckled at edges, which indicated the poor adhesion of the films to the substrate. The wrinkles spread into the films with the increase in the time and is attributed to the relaxation of stresses in the

films over time. It can be inferred that buckling is due to high compressive stresses developed in the films during the deposition.

4.1.1 Raman Spectroscopy

It is a known fact that for a tetrahedral amorphous carbon film, a broad peak centered at a Raman shift of 1570cm^{-1} is observed. A peak at 1350cm^{-1} is due to the D band corresponding to the disordered graphite.

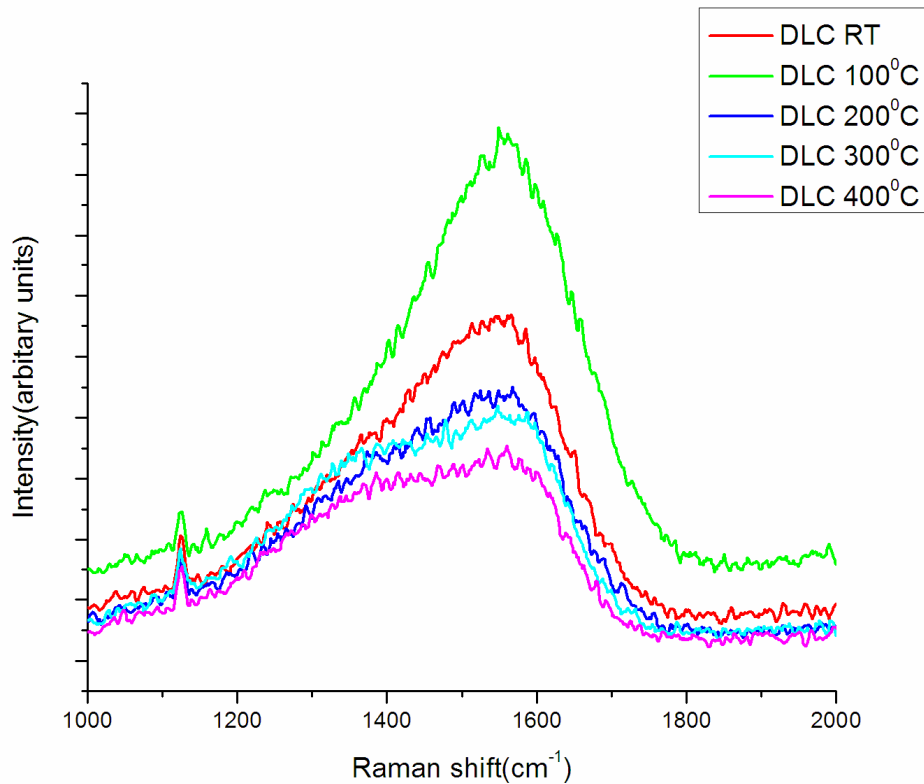


Figure 4.1 Raman Spectra of the Tetrahedral Amorphous Carbon Films Deposited at Different Temperatures

Figure 4.1 shows the Raman spectra for the films deposited at various temperatures. If the shoulder at 1350 cm^{-1} is less, it implies that the film has more sp^3 content. The film deposited at room temperature, 100°C does not show a prominent peak at 1350 cm^{-1}

indicating the presence of higher sp^3 fraction than sp^2 . Even the film deposited at 200°C did not show a significant peak at 1350 cm^{-1} . As the deposition temperature is increased from 200°C to 400°C, the films exhibited a hump at 1350 cm^{-1} and the width of the shoulder increased. This indicates the decrease in the sp^3 fraction and hence can be concluded that the films exhibit more graphitization, as seen from the Raman spectra. From the Raman Spectroscopy, it can be inferred that there is a decrease in the sp^3 content with the increase in the deposition temperature. If the amorphous carbon films exhibit a high content of sp^3 bonding they are addressed as tetrahedral amorphous carbon films. From the Raman spectra it is confirmed that these films exhibit a high content of sp^3 and hence can be termed as tetrahedral amorphous carbon films (ta-C). Here after this notation is used for all the films.

Raman Spectroscopy was used to determine the stresses in the films. The equilibrium separation between the atoms change with the increase in the stresses and this in turn changes the vibrational frequencies. This change can be observed in the Raman shift. If the atoms are under tension, the vibrational frequencies decrease and hence the Raman shift decreases. The atoms in the compression exhibit an increase in the vibrational frequencies and the Raman shift increases. The stresses developed in the films can be calculated using

$$\sigma = E \left(\frac{\Delta\omega}{\omega} \right)$$

$\Delta\omega$ = Shift in the Raman wave number

ω = wave number of the reference

E= elastic modulus of diamond-like carbon

Table 4.1 gives the reduction in the stress in ta-C films without interlayers, calculated using the G-band at 1570 cm⁻¹ as the reference. The peaks were obtained using a multiple peak Gaussian fit. With the increase in deposition temperature, the peak shifted to the left, indicating a decrease in the stress, which is evident from the decrease in the stress values given in the Table 4. 1. The modulus value is assumed as 412GPa for the calculations.

Table 4. 1 Residual Stress in the Tetrahedral Amorphous Carbon Films Obtained from Raman Spectra

Sample	Deposition Temperature (°C)	Residual Stress (GPa)
DLC	RT	1.892
DLC	100	1.664
DLC	200	2.294
DLC	300	2.602
DLC	400	6.2522

4.1.2 Nanoindentation

It is important to retain the hardness of DLC films while making efforts to improve its other properties. Nanoindentation is the best technique to measure the mechanical properties of thin films like hardness and modulus. Berkovich diamond tip was used as the indenter. Nine indents were performed on each sample at different locations using Nanoindenter XP. To reduce any errors in the calculations the average values of hardness and modulus were accepted. The modulus and hardness values were obtained using Oliver and Pharr's approach. For every set of experiment, indentations were also performed on fused Silica to confirm that the tip is in perfect shape.

Figure 4.2 and Figure 4.3 shows the variation of modulus and hardness with the indenter displacement. From the nanoindentation test, it was observed that with the increase in the temperature, the hardness and the modulus of the ta-C films increase up to a temperature of 100° C and then starts to decrease in the entire range. This is because of the increase in the sp^2 bonds at higher temperatures, which was earlier confirmed from the Raman spectra. The films deposited at 100° C exhibited high fraction of sp^3 content and hence has the highest hardness and modulus value. The values of young's modulus and hardness were obtained using Oliver and Pharr's approach and the results are summarized in Table 4.2.

Table 4.2 Hardness and Young's Modulus for Tetrahedral Amorphous Carbon Films Deposited at Various Temperatures

Sample	Deposition Temperature(°C)	Young's modulus (GPa)	Hardness(GPa)
Sample 1	Room Temperature	370.096	51
Sample 2	100	412.784	59.320
Sample 3	200	363.947	43.451
Sample 4	300	250.721	22.493
Sample 5	400	198.264	16.473

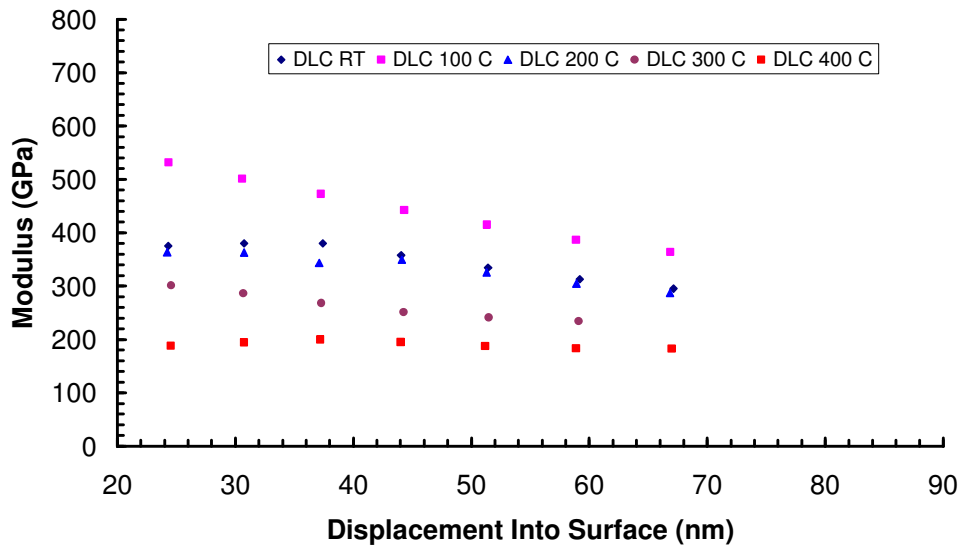


Figure 4.2 Modulus vs Displacement Plot of Tetrahedral Amorphous Carbon Films Deposited at Different Temperatures

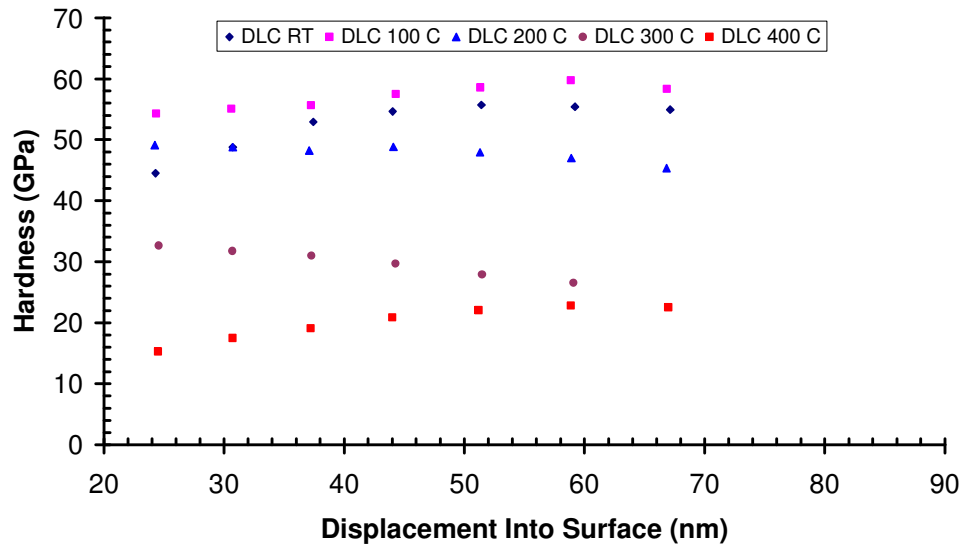


Figure 4.3 Hardness vs Displacement Plot of Tetrahedral Amorphous Carbon Films Deposited at Different Temperatures

4.2 Tetrahedral Amorphous Carbon Films with Interlayer

The delamination of the ta-C films due to high compressive stresses is an obstacle for its application. These stresses can be reduced either by increasing the deposition temperature or by decreasing the energy of carbon species. However, from the discussion in earlier section, it is evident that the increase in the deposition temperature results in the graphitization of the films. The films with higher sp^2 content exhibit a lower hardness, which is not desirable. The stresses in thin films are reduced efficiently by using interfacial layers, materials that can form carbides and which exhibit lower stresses at the interface are the best materials as interlayers. To serve as an efficient interlayer, the modulus of such materials should lie between the modulus of the substrate and the deposited films.

This section discusses the enhancement in the adhesion of ta-C films with the substrate by the presence of interlayer. Carbides, nitrides and metals that have affinity for carbon were used as interfacial layers. Using PLD, compounds such as TiC, TiN, AlN, TaN, and metals like Ta and W were deposited as interfacial layers. The stresses in the interface materials vary with the deposition temperature and hence the investigation was done at three different deposition temperatures of 100°C, 300°C, and 600°C. The deposition was carried out for 20 minutes. For all the samples, the tetrahedral amorphous carbon was deposited on these interfaces at 100°C because the as deposited samples have shown higher sp^3 content at this temperature. This particular temperature was opted because the undoped ta-C at this temperature exhibited high fraction of sp^3 bonds. With the aid of the multiple target holders, the required multilayer thin films were successfully deposited. The results of Raman spectroscopy, Nanoindentation and friction test are discussed in the following sections.

4.2.1 Raman Spectroscopy

Raman spectra of these samples revealed that with the increase in deposition temperature of interlayer, the G-peak moved towards left, indicating the relaxation of stresses in the films. All the selected interlayer materials followed the same trend. Figure 4.4 shows the Raman spectra of ta-C films with tantalum as interlayer. From the Figure 4.4 it can be observed that there is no significant D-peak at 1350 cm^{-1} indicating that the films are predominantly sp^3 bonded.

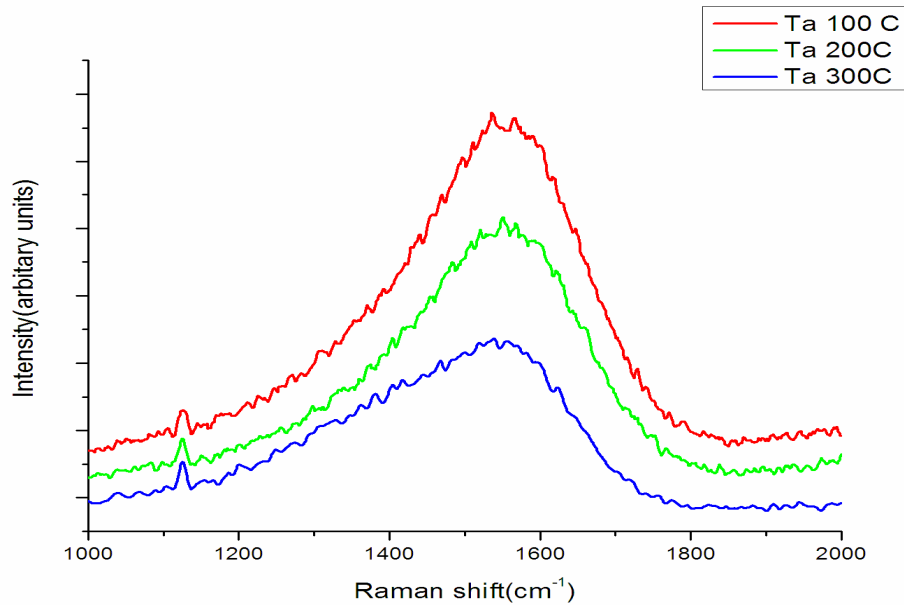


Figure 4.4 Raman Spectra of ta-C films with Ta as Interfacial Layer

High quality ta-C films exhibit a relatively symmetric G-band and a very less significant D-band in the Raman spectra. The following figures show the Raman spectra of ta-C films with the interlayers deposited at different temperatures. The G-band for all the spectra was located using multiple Gaussian fit. The reduction in stress in ta-C films were calculated by measuring the shift in the peaks and the resulting values for all the films are summarized in the Table 4.3. For the calculations, modulus of diamond-like carbon is taken as 412 GPa.

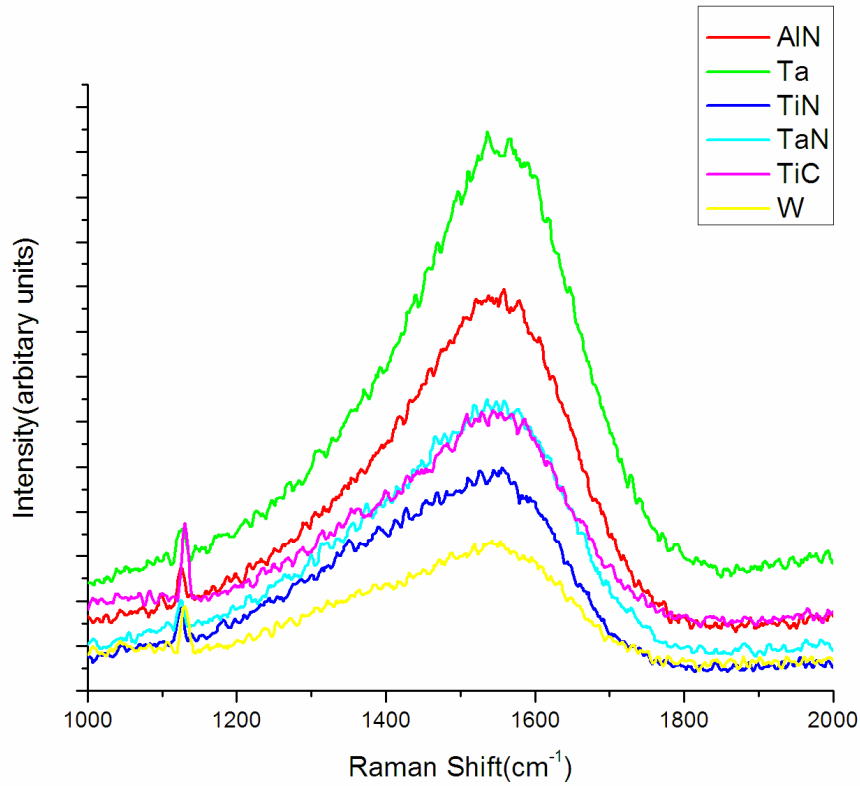


Figure 4.5 Raman Spectra of ta-C Film with Different Interlayers Deposited at 100°C

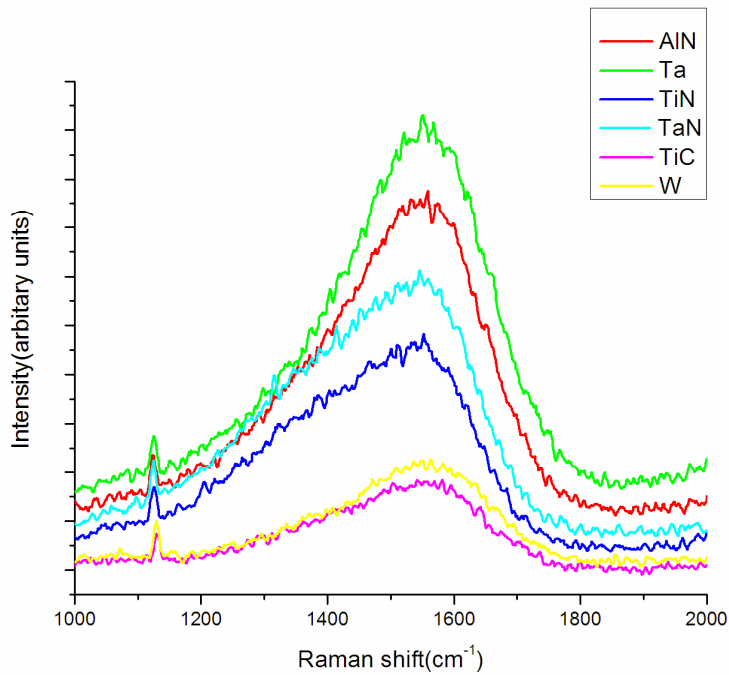


Figure 4.6 Raman Spectra of ta-C Film with Different Interlayers Deposited at 300°C

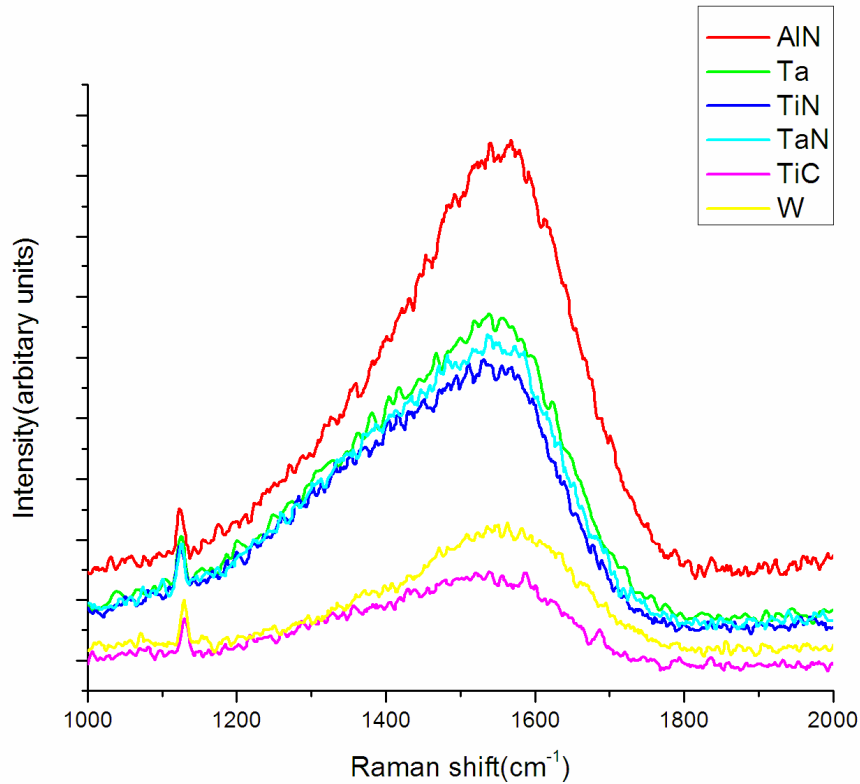


Figure 4.7 Raman Spectra of ta-C Film with Different Interlayers Deposited at 600°C

ta-C films with AlN as an interlayer did not show change in the compressive stress with the change in the deposition temperature. ta-C with Ta as interface exhibited a considerable amount of reduction in stresses at high deposition temperature of Tantalum. The stress reduction was more in the films with TiN as the interface. Films with TiC interlayer, deposited at 600°C exhibited the maximum reduction in the stress.

Table 4.3 Reduction in Stress (GPa) Obtained from Raman Analysis

Sample	Interlayer material	Deposition temperature (°C)	G-band (cm ⁻¹)	Residual stress (GPa)
Sample 6	AlN	100	1549.06	2.71
Sample 7	AlN	300	1548.97	2.72
Sample 8	AlN	600	1553.66	1.49
Sample 9	Ta	100	1557.08	0.59
Sample 10	Ta	300	1556.81	0.58
Sample 11	Ta	600	1542.64	4.41
Sample 12	TiN	100	1542.72	4.38
Sample 13	TiN	300	1540.18	5.06
Sample 14	TiN	600	1539.37	5.27
Sample 15	TaN	100	1544.26	3.97
Sample 16	TaN	300	1543.80	4.1
Sample 17	TaN	600	1542.79	4.36
Sample 18	TiC	100	1549.54	2.57
Sample 19	TiC	300	1548.23	2.92
Sample 20	TiC	600	1538.92	5.39
Sample 21	W	100	1543.8	4.1
Sample 22	W	300	1546.82	3.30
Sample 23	W	600	1542.67	4.39

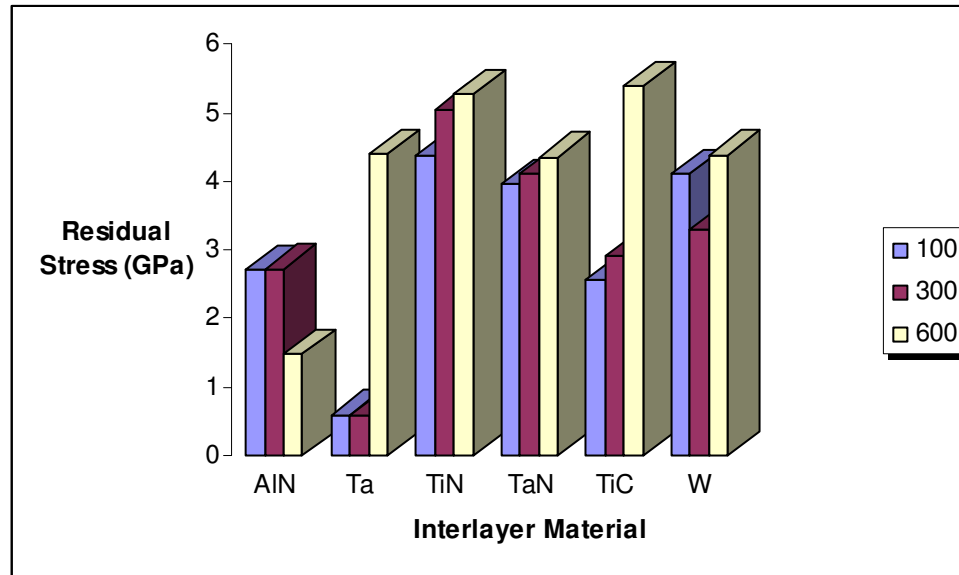


Figure 4.8 Reduction in Stress vs Interlayer Material at Different Temperatures

4.2.2 Nanoindentation

The hardness and the modulus of all the samples were tested using Nanoindenter XP and the results were summarized in Table 4.4. The plots of modulus vs displacement and hardness vs displacement were also included. Of all the samples, films with TiN as interlayer exhibited highest hardness. All the films exhibited almost same hardness owing to the fact that all the selected interlayers are hard materials.

Table 4.4 Summarized Results Obtained from Nanoindentation for Layered Tetrahedral Amorphous Carbon Films

Sample	Interlayer Material	Deposition temperature(°C)	Young's Modulus(GPa)	Hardness(GPa)
Sample 6	AlN	100	248.353	25.143
Sample 7	AlN	300	240.265	24.542
Sample 8	AlN	600	269.077	26.267
Sample 9	Ta	100	224.831	28.023
Sample 10	Ta	300	258.793	27.731
Sample 11	Ta	600	248.675	25.75
Sample 12	TiN	100	329.536	29.454
Sample 13	TiN	300	306.367	31.909
Sample 14	TiN	600	289.879	28.122
Sample 15	TaN	100	208.798	27.104
Sample 16	TaN	300	293.346	26.653
Sample 17	TaN	600	200.872	25.738
Sample 18	TiC	100	217.172	26.974
Sample 19	TiC	300	221.542	25.115
Sample 20	TiC	600	245.854	26.165
Sample 21	W	100	237.266	28.02
Sample 22	W	300	224.166	26.021
Sample 23	W	600	194.416	24.056

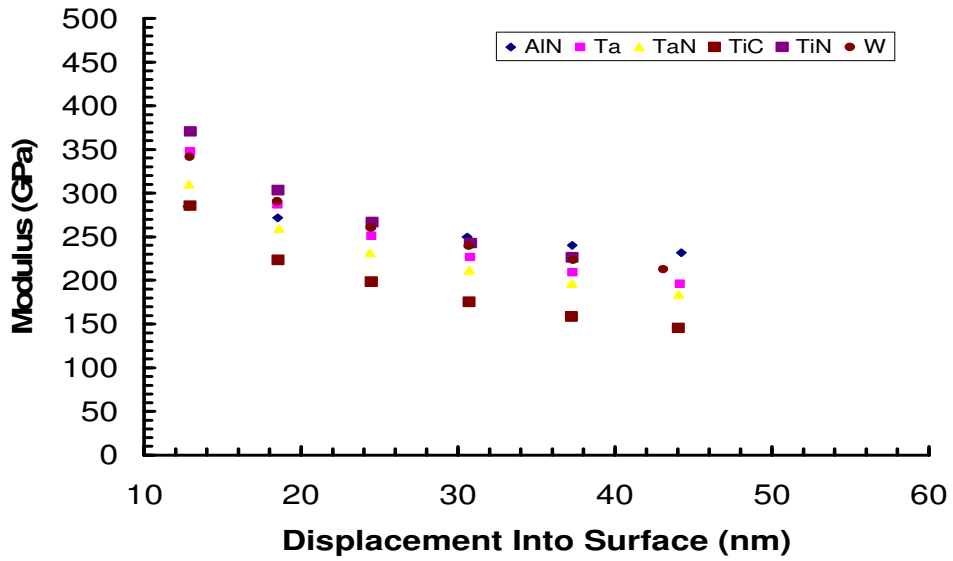


Figure 4.9 Modulus vs Displacement Plot of ta-C Film with the Interlayers Deposited at 100°C

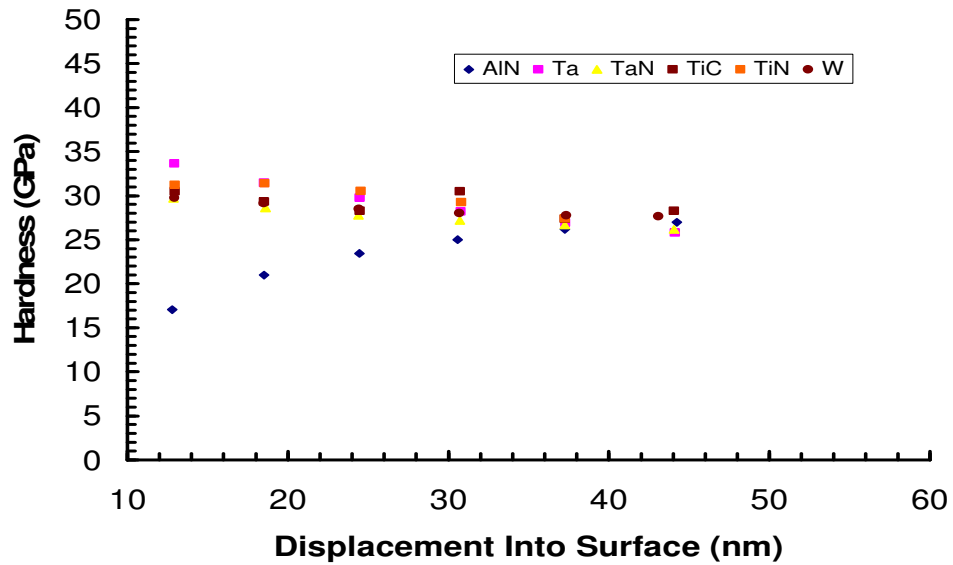


Figure 4.10 Hardness vs Displacement Plot of ta-C Film with the Interlayers Deposited at 100°C

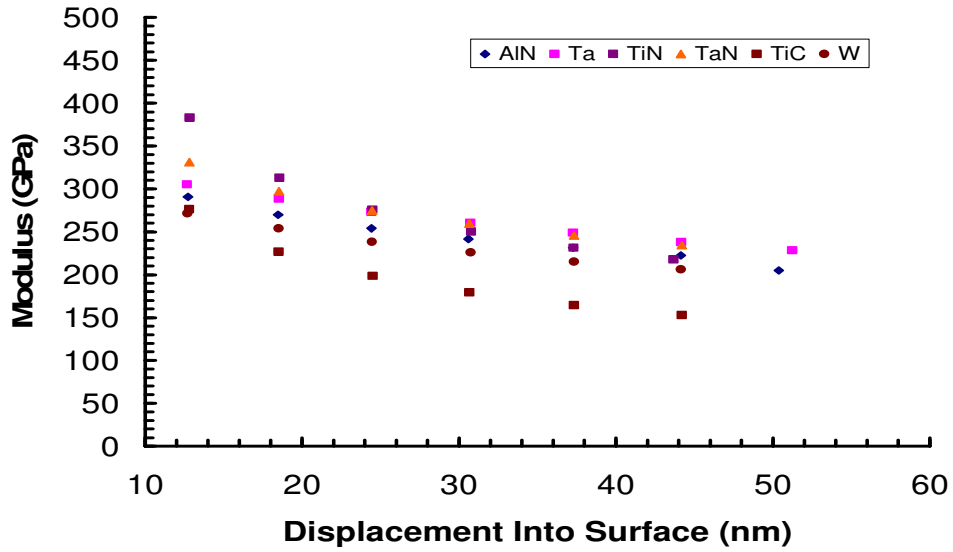


Figure 4.11 Modulus vs Displacement Plot of ta-C Film with the Interlayers Deposited at 300°C

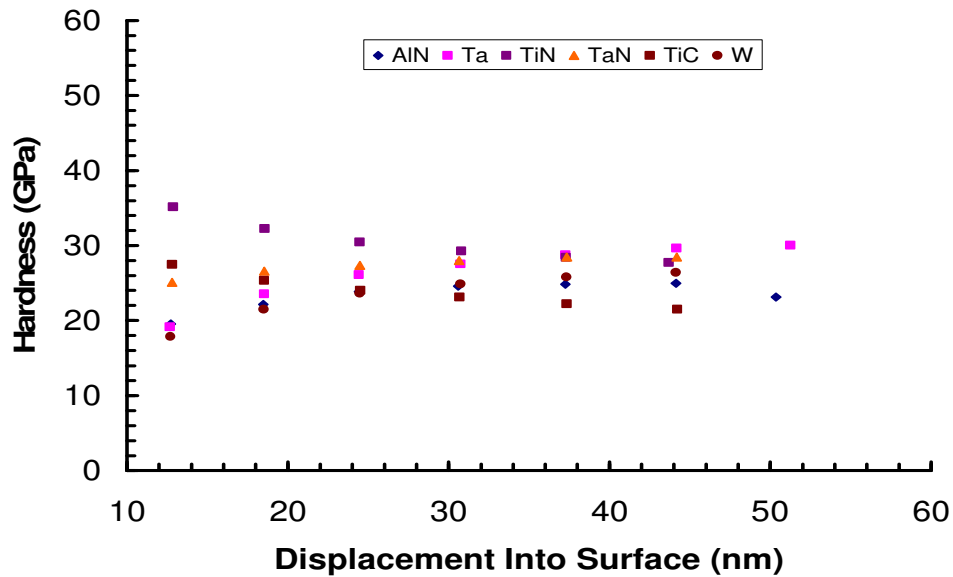


Figure 4.12 Hardness vs Displacement Plot of ta-C Film with the Interlayers Deposited at 300°C

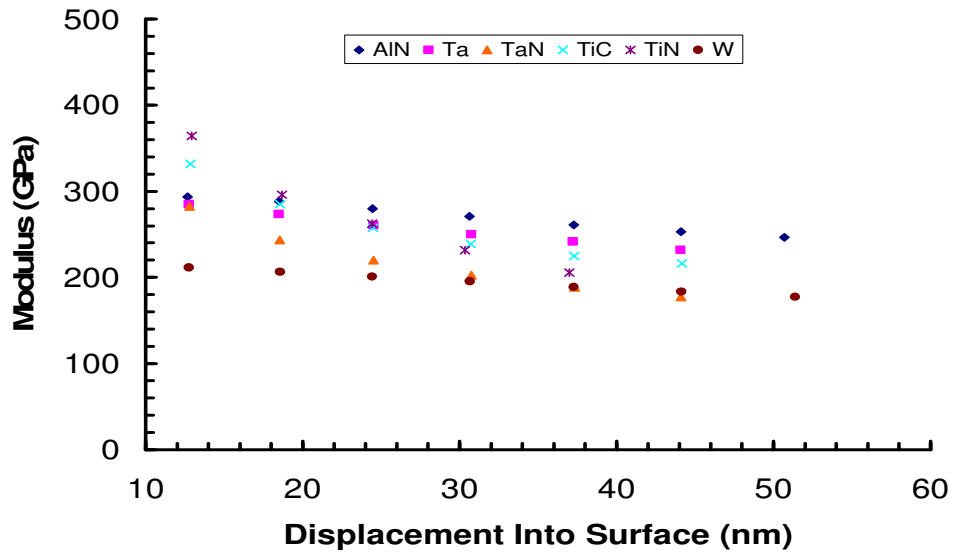


Figure 4.13 Modulus vs Displacement Plot of ta-C Film with the Interlayers Deposited at 600°C

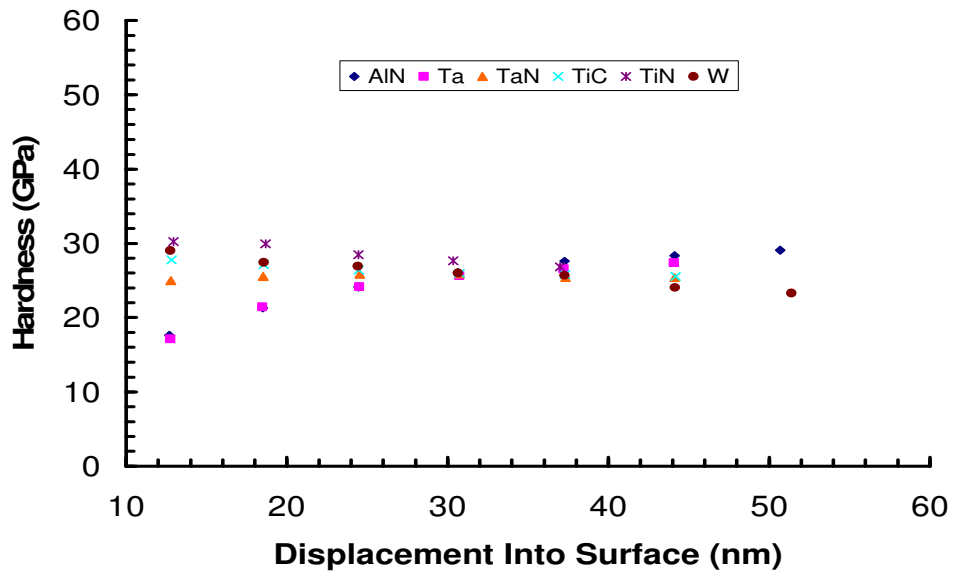


Figure 4.14 Hardness vs Displacement Plot of ta-C Film with the Interlayers Deposited at 600°C

4.2.3 Friction Test

Using the ball on disk method, friction test was performed on all the samples against stainless steel balls. A load of 4N was applied for one minute at a translational velocity of 2mm/sec. As deposited ta-C films that were tested with UMT against stainless steel ball, demonstrated a coefficient of friction of 0.02. From the test results, it was observed that the coefficient of friction of the ta-C films deposited on interlayers decreased with the lowest being exhibited by the films with TaN interlayer. The table below summarizes the friction test results.

Table 4.5 Friction Coefficient of Layered ta-C Films

Sample	Interlayer Material	Deposition temperature(°C)	Friction coefficient
Sample 6	AlN	100	0.013
Sample 7	AlN	300	0.014
Sample 8	AlN	600	0.012
Sample 9	Ta	100	0.010
Sample 10	Ta	300	0.018
Sample 11	Ta	600	0.014
Sample 12	TiN	100	0.016
Sample 13	TiN	300	0.014
Sample 14	TiN	600	0.012
Sample 15	TaN	100	0.014
Sample 16	TaN	300	0.011

Table 4.5 (continued)

Sample 17	TaN	600	0.018
Sample 18	TiC	100	0.019
Sample 19	TiC	200	0.017
Sample 20	TiC	300	0.012
Sample 21	W	100	0.015
Sample 22	W	200	0.017
Sample 23	W	300	0.019

4.3 Diamond

In order for the stresses in diamond film to be minimum, the difference in the coefficient of thermal expansion of the substrate and the film should be as low as possible. Intrinsic stresses are developed during the growth of the films due to the impurities in the layer whereas the thermal stresses are developed when the sample is cooled to room temperature rapidly. The diamond coatings on Ti-6Al-4V alloy, mostly used in aerospace airframe, engine parts, and bone implants, were investigated in this research. This alloy exhibits poor adhesion with the diamond films and hence the effect of interlayers on the improvement of adhesion is studied.

Initially, diamond is deposited on Ti-4Al-6V substrate. The film has peeled off due to the adhesion problems arising because of the mismatch of coefficient of thermal expansion. Adhesion of these films can be enhanced by using an interlayer that induces chemical or mechanical bonding between the diamond and the substrate. The interlayer should

provide a transition of modulus and thermal expansion coefficient from substrate to the diamond film, which reduces the stresses.

TiN and TiC were investigated as the interlayers to enhance the adhesion of diamond films on Ti-4Al-6V alloy. The experimental procedure was discussed in section 2.2.2. Raman spectroscopy and XRD were used to characterize the structural properties of the films.

4.3.1 Raman Spectroscopy

Raman spectroscopy was performed on the diamond films deposited on Ti-6Al-4V with TiC and TiN interlayers. Raman peak of diamond on bare silicon substrate is taken as reference. Figure 4.15 shows the Raman spectra of diamond on bare silicon and on other interlayers. The diamond peak on Si was obtained at 1332.57 cm^{-1} . The samples with TiN as an interlayer demonstrated a peak at 1345.71 cm^{-1} and 1570 cm^{-1} . The peak at 1332.57 cm^{-1} , attributed to diamond (sp^3 bonding), shifted to 1345.71 cm^{-1} indicating the presence of high compressive stresses. The peak at 1570 cm^{-1} is attributed to sp^2 bonding and indicates the presence of graphite. Diamond films with TiC interlayer have shown a minor shift in the peak from 1332.57 cm^{-1} to 1333.4 cm^{-1} . Hence, these samples have less compressive stresses compared to the TiN films. Stresses developed in these films was calculated using the Raman shift. Considering the modulus of diamond deposited on silicon, which in this case is 900GPa, the increase in stresses was calculated. The values are summarized in Table 4.5.

Table 4.6 Increase in Stress (GPa) Obtained from Raman Analysis

Outer Layer	Interlayer material	Raman shift(cm^{-1})	Increase in Stress(GPa)
Diamond	TiC	1333.4	0.56
Diamond	TiN	1345.71	8.87

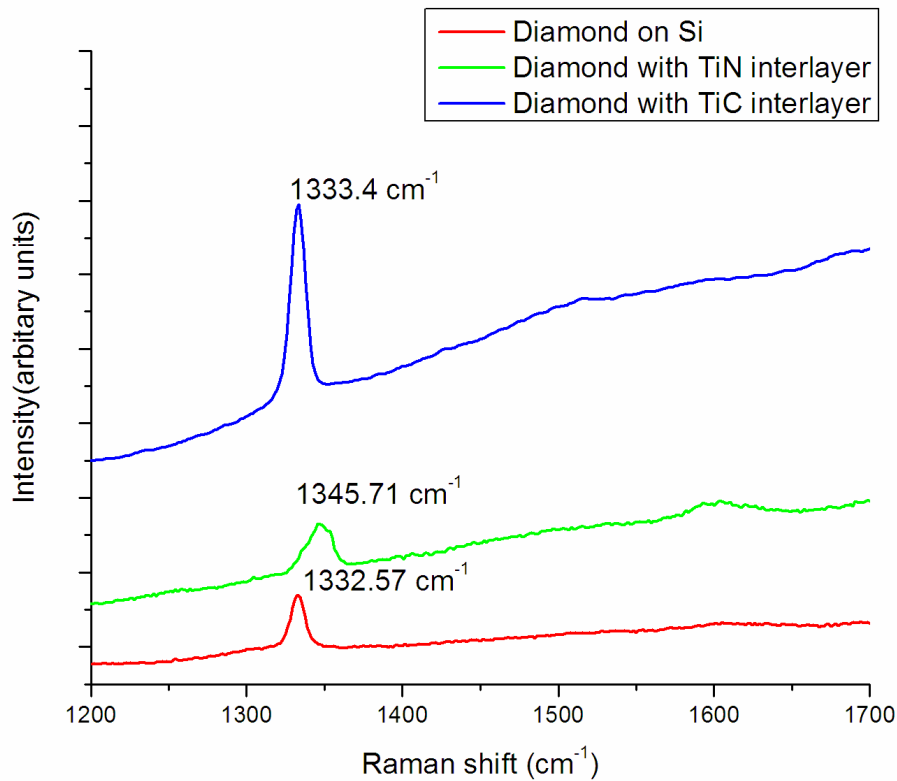


Figure 4.15 Raman Spectra of Diamond Films with Different Interfaces

4.3.2 X-ray Diffraction

In order to improve the adhesion of the films, a thick coating of TiN and TiC were deposited using PLD. Diamond films on TiN did not adhere well at the edges, whereas the TiC interlayer resulted in good adhesion of diamond films on Ti alloy substrate.

Figure 4.16 shows the XRD pattern of the substrate and the TiC interlayered diamond film. Peaks corresponding to TiC and diamond are represented in Figure 4.16.

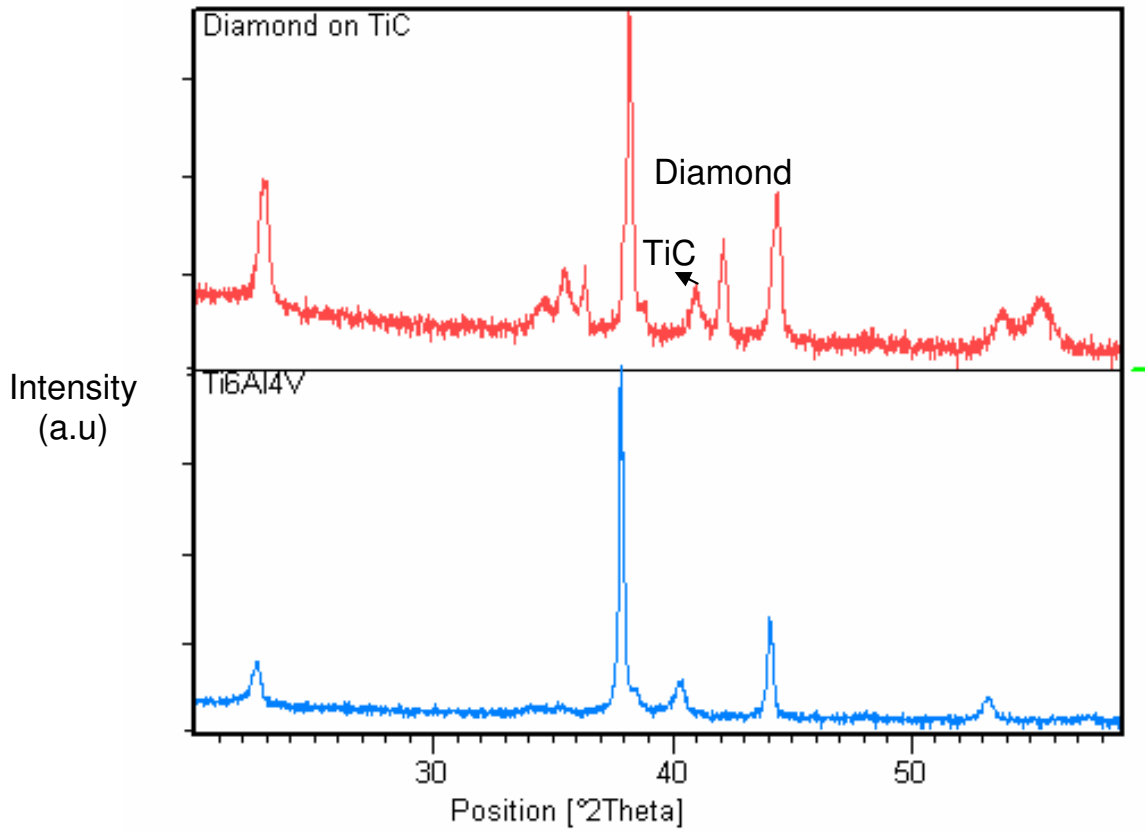


Figure 4.16 XRD of Original Substrate and TiC –Diamond Film

CHAPTER 5

CONCLUSIONS AND RECOMMENDATIONS

Compressive stresses, poor adhesion, and poor wear resistance are found to be the crucial factors with the tetrahedral amorphous carbon and diamond films that are extensively used in the microelectronic device packaging, cutting tools and wear resistant magnetic disks. The interfacial bonding and internal stresses determine the adhesion of thin films. This research investigated the growth and characterization of diamond and diamond-like materials on Ti alloy and Silicon substrates, particularly to improve the adhesion by reducing the internal stresses. Tetrahedral amorphous carbon (ta-C) primarily contains the sp^3 bonds and has properties close to diamond. The hardness of as deposited ta-C films decreased with the increase in the deposition temperature because of the increase in the sp^2 character at higher temperatures. Raman analysis revealed a decrease in the internal stress with the increase in the deposition temperature but at the same time, the D-band corresponding to the sp^2 content in the films has become significant.

An interlayer that has affinity to form carbide with a modulus value between tetrahedral amorphous carbon and silicon has the potential to reduce the internal stresses. Films with TiN interlayer, deposited at 300°C and 600°C has the maximum stress reduction of 5.06 and 5.27 GPa respectively. The nanoindentation tests on these samples revealed that they did not exhibit any significant change in the hardness values with the change in the

deposition temperature of interlayers. Film with TiC interlayer deposited at 600°C, also exhibited a stress reduction of 5.39 GPa. Hence, the interlayers of TiN at 300°C and 600°C, TiC at 600°C can be considered to have the potential to reduce stresses in the ta-C films. Friction test results demonstrate a decrease in the coefficient of friction of the interlayered ta-C films.

Diamond films grown on the Ti-6Al-4V were peeled off due to high interfacial stresses. The adhesion of these films was improved with an interlayer of TiN and TiC. The Raman spectra of these films have revealed that the compressive stresses are more with a TiN interface when compared to TiN interface. XRD was used to study the microstructure of these films. The peak corresponding to diamond and TiC were observed in the XRD results.

The future for diamond and diamond-like carbon films is bright in orthopedic applications. With low friction coefficient and improved adhesion diamond-like carbon films and diamond can be efficiently used in joint replacement for improving the mechanical properties of bulk material and hence enhancing the integration with the bone.

REFERENCES

- [1] A.A. Voevodin, J.P. O'Neill and J.S. Zabinski, "Tribological performance and tribochemistry of nanocrystalline WC/amorphous diamond-like carbon composites", *Thin Solid Films*, Volume 342 (1999), pages 194-200.
- [2] A. A. Voevodin, S. D. Walck and J. S. Zabinski, "Architecture of multilayer nanocomposite coatings with super-hard diamond-like carbon layers for wear protection at high contact loads", *Wear*, Volumes 203-204, March 1997, Pages 516-527.
- [3] C. Donnet, J. Fontaine, T. Le Mogne, M. Belin, C. Héau, J. P. Terrat, F. Vaux and G. Pont, "Diamond-like carbon-based functionally gradient coatings for space tribology", *Surface and Coatings Technology*, Volumes 120-121, November 1999, Pages 548-554.
- [4] Paolo Mosaner, Marco Bonelli and Antonio Miotello, "Pulsed laser deposition of diamond-like carbon films: reducing internal stress by thermal annealing", *Applied Surface Science*, Volumes 208-209, 15 March 2003, Pages 561-565.
- [5] D. K. Sood, W. R. Drawl and Russell Messier, "The effect of carbon ion implantation on the nucleation of diamond on Ti-6Al-4V alloy", *Surface coating technologies*, 51(1-3): 307-312, 1992.
- [6] Yongqing Fu, Hejun Du and Chang Q. Sun, "Interfacial structure, residual stress and adhesion of diamond coatings deposited on titanium", *Thin Solid Films*, Volume 424, Issue 1, 22 January 2003, Pages 107-114.
- [7] Helena Ronkainen, "Tribological properties of hydrogenated and hydrogen free diamond-like carbon coatings", *Dissertation*, Technical research centre of fenland, 2001.
- [8] A.C.Ferrari and J.Robertson, "Interpretation of Raman spectra of disordered and amorphous carbon", *Physical review B*, 1999, volume 61, number 20.
- [9] Lacerda, R.G. and F.C. Marques, "Hard Hydrogenated Carbon Films with Low Stress", *Applied Physics Letters* 73 (1998) 617-619.
- [10] Dekempeneer, E.H.A., R. Jacobs, J. Smeets, J. Meneve, and L. Eersels "R.F. Plasma-Assisted Chemical Vapor Deposition of Diamond-Like Carbon: Physical and Mechanical Properties" *Thin Solid Films* 217 (1992) 56-61.
- [11] Robertson, J., 1986 *Adv Phys.*35,317.

- [12] Namwoong Paik, “Raman and XPS studies of DLC films prepared by a magnetron sputter-type negative ion source”, Surface and Coatings Technology, In Press, Corrected Proof, Available online 18 September 2004.
- [13] J.Cheung and J.Horwitz, “Pulsed laser deposition history and laser-target interactions”, MRS bulletin, 1992, volume 25, No.2.
- [14] Foltyn.S.R., Dye.R.C., K.C.Ott, K.M.Hubbard, W.hutchinson, R.E.Muenchausen, R.C.Esler, and X.D.Wu, Appl.PHYS Lett.59, 594.
- [15] Kools, J.C.S, C.J.C.M.Nillesen, S.H.Brongersma, E. Van de reit, and, J.Dieleman, J.Vac.Sci and technology, A10, 1809(1992).
- [16] Holzapfel,B., B.Roas,L.Schultz, P.Bauer, and G.Saemann-Ischencko, Appl.phys.lett.61 ,3178(1992).
- [17] J.levoska, s.leppavuori, applied surface science 86(1995) 180-184.
- [18] W. Kaiser and W. L. Bond Bell “Nitrogen, a major impurity in type I diamond” Telephone Laboratories, Murray Hill, New Jersey.
- [19] G.M.Pharr, W.C.Oliver, F.R.Brotzen, “On the generality of the relationship among contact stiffness, contact area, and elastic modulus during indentation”, J.Mater.Res, Vol.7.No.3, Mar 1992.
- [20] A. C. Fischer-Cripps “A review of analysis methods for sub-micron indentation testing Vacuum” Volume 58, Issue 4, September 2000, Pages 569-585.
- [21] http://www.matter.org.uk/diffraction/x-ray/x_ray_diffraction.htm#.
- [22] Karl E Spear, John P. Dismukes, “Synthetic diamond: emerging CVD science and Technology”, Wiley publication, 1994.
- [23] Robert E. Clausing, Linda L. Horton, John C. Angus, Peter Koidl, “Diamond and diamond-like films and coatings”, Plenum publication, 1991.
- [24] Deryagin, B.V., and Fedoseev, D.V., Russian Chem. Rev, 39, 783, 1970.
- [25] S.Aisenberg and R.Chabot “ Ion beam deposition of thin films of diamond-like carbon”, Journal of applied physics, vol 42, 2953, 1971.
- [26] <http://pubs.usgs.gov/of/of01-041/htmldocs/images/beam.jpg>